

# Test Summary of the Full-Span High-Lift Common Research Model at KHI aero-acoustic Low-Speed Wind Tunnel

Takahiro Hashioka <sup>1</sup>, Yoshiki Murahashi <sup>1</sup>, Hidemasa Yasuda <sup>1</sup>, Yuta Sawaki <sup>1</sup>,

Sho Onda<sup>1</sup>, Yuta Tsuchimoto<sup>1</sup>, Yusuke Nishizaki<sup>1</sup>, Wataru Suzuki<sup>1</sup> & Takeo Kawamura<sup>1</sup>.

<sup>1</sup>Kawasaki Heavy Industries, Ltd., Kakamigahara, Gifu, 504-8710, Japan Aerodynamic Engineering Section

## **Abstract**

Kawasaki Heavy Industries, Ltd. (KHI), an aircraft company in Japan, built the 3 x 3m Kawasaki Low-speed aero-acoustic Wind Tunnel (KLWT) in 2017 - 2019 to replace the old wind tunnel built in 1938. KHI introduced 3.23% High-speed and High lift Common Research Model (CRM-HS and CRM-HL) as a check standard model for the quality assurance of this new KLWT in 2019 to 2022 and tested it in Oct. 2022 and Jan. 2023 with full support and participant of CRM-HL Ecosystem team. In this paper, after short introduction of KLWT and KHI CRM-HL model, the test results of reference landing configuration are presented with related CFD results done in order to assess the support and wall interferences.

Keywords: CRM-HL, Wind tunnel, CFD, EFD

#### Introduction

In the CRM-HL Ecosystem [1-9], Computational Fluid dynamics (CFD) engineers and Experimental Fluid Dynamics (EFD) engineers from various organizations are working together to prepare a rich set of experimental data for the CFD validation dialogue, exploring the proper ways for coexistence of CFD and EFD in the developments, and aiming for sustainable future with environment friendly aircrafts.

KHI fortunately met with CRM [10-12]/CRM-HL [1] during the new low-speed wind tunnel (KLWT) project and selected it as a check standard model for KLWT. For KHI team, everything related with CRM/CRM-HL started from here, and now our CFD/EFD members are also working in the Ecosystem.

This paper describes the KHI (section 1) and KLWT (section 2), KHI-CRM-HL (section 3), test setup/results of KHI CRM-HL model at KLWT (section 4) and the future plan (section 5).

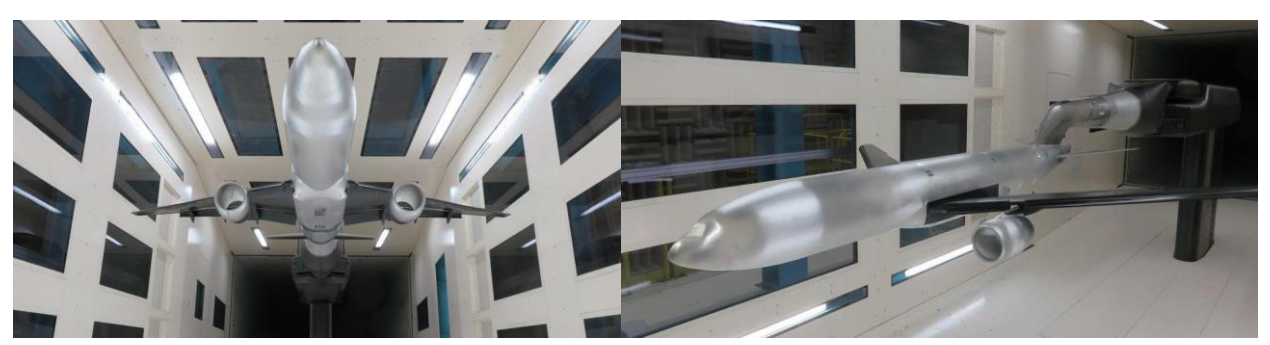


Figure 1 – KHI CRM-HL at KLWT

# 1. Company and facilities

Firstly, KHI and its facilities are introduced in this section.

#### 1.1 KHI

KHI originated as a ship builder in 1878 and now is a units of manufacturing companies in Japan. KHI is manufacturing various types of platforms of the transportation and infrastructures including ships, trains, motorcycle, aircrafts, jet engines, gas turbines, robots, and the shield machines, etc.



Figure 2 – KHI products

### 1.2 KHI Gifu works

KHI Aerospace Systems Company, one of KHI group companies, is manufacturing various aircrafts and related parts at Gifu and Nagoya works for both commercial and defense markets. Figure below shows the examples of products of these works. KHI basically develops an aircraft and related systems by ourselves but sometimes develops those with both domestic and foreign partners cooperatively.



<sup>\*1:</sup>Carrier,First flight in 2010, \*2:Maritime patrol aircraft,First Flight in 2007, \*3:Trainner aircraft,First Flight in 1985 Figure 3– KHI Gifu and Nagoya works products

## 1.3 KHI wind tunnels in Gifu works

For aircraft development and research, there are two wind tunnels in KHI Gifu works, one of them is High speed wind tunnel (Kawasaki Transonic Wind Tunnel, KTWT) that is blow-down type pressurized transonic wind tunnel with 1[m] square test section and its Mach range is from 0.2 to 1.4.

And the other is low speed one (KLWT) where the KHI CRM-HL test was done and detail information on it will be described in the next section.





KTWT(1988-) KLWT(2019-) Figure 4– KHI wind tunnels in Gifu works

## 2. KLWT

Here, a basic and brief description of KLWT is given.

# 2.1 Background history

In KHI Gifu works, there was an old low-speed wind tunnel built in 1938 and that tunnel was used over 80 years for the developments of various Japanese aircrafts including fixed wing aircrafts, rotor crafts and projectiles shown in previous page. However, it became too old and restrictive to fulfill the requirements of future expected tests and also too fragile to endure a huge earthquake that may happen in Japan, so in order to replace the old tunnel, new low-speed wind tunnel was planned and designed in 2010 to 2016 and built in 2017 to 2019. For this wind tunnel, acoustic testing capability was added considering the future needs for the acoustic tests to reduce the environmental impact of the aircrafts especially. This new wind tunnel is current KLWT, and its construction completed on Mar.2019. KLWT started its operation from Mar.2020 after 1-year flow calibration testing campaign.





OLD KLWT(1938-2022)

(new/current) KLWT(2019-)

Figure 5 – KLWT history

# 2.2 KLWT Specification

Current KLWT is designed and manufactured by KHI as an atmospheric(non-pressurized) and continuous (Göttingen) type wind tunnel with acoustic testing capability. KLWT is driven by 4[MW] electric motor powered by the latest matrix converter with high efficiency. Total 160[m] long flow circuit of KLWT is set horizontally on the ground and it consists of test section,  $1^{st}$  diffuser, corner vanes fan/motor,  $2^{nd}$  diffuser, heat exchanger, setting chamber with flow conditioners (1 flow straightener honeycomb/ 3 screens for flow uniformity) and contraction (nozzle) as shown in Figure 6. Basic test section size is 3.0[m] wide, 3.0[m] height and 9.0[m] long but by sliding the sidewalls outside parallelly, its width is changeable from 3 to 4[m] for a test with high blockage model. Maximum flow speed is 102[m/s] (Mach=0.3) and flow temperature can be controlled within  $\pm 1$  [°C] of ambient temperature by water flowing through long slender pipes of the heat exchanger. Setting chamber is 9.0[m] square and contraction ratio is 9.0 for 3[m] width and 6.8 for 4[m] width configuration. Regarding the closed test section, side walls are slightly diverging to compensate the boundary layer thickness increase for the negligible stream wise velocity gradient. Table below shows the representative specifications of KLWT.

Table 1– KLWT specifications

1	Wind tunnel Type	Continuous (Göttingen type)	Enviromental pressure	Atmospheric (not pressurized)
2	Willa tuiller Type	(closed return circuit)	Drive Motor Power	4[MW]
3	Test Section Type	(1) Closed (2) Open	Model Support System	(1) Sting Support (2) Strut Support
4	Test Section Size	W3.0 × H3.0 × L9.0[m] W4.0 × H3.0 × L9.0[m]	Contraction ratio	9.00 for W3.0[m] 6.75 for W4.0[m]
5	Maximum Velocity	~102 [m/s]@Closed ~ 85 [m/s]@Open	Backgrond Noise	≤ 80 [dB(A)] (85[m/s], W3.0[m])

NOTE: Typical test section size and flow velocity of old wind tunnel was W2.5[m] by H2.5 [m] and 40-50[m/s].

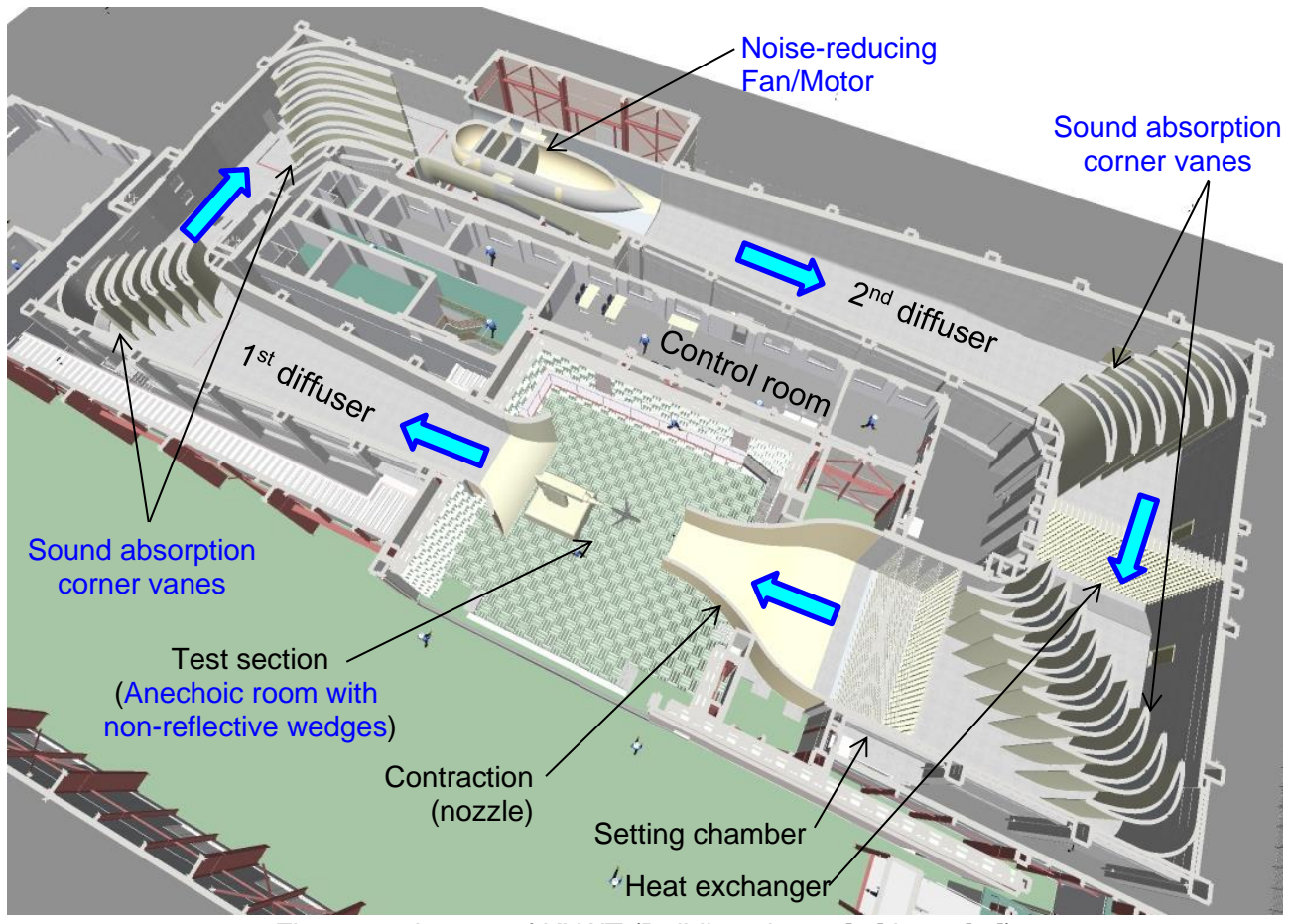


Figure 6 – Layout of KLWT (Building size 90[m] by 51[m])

Figure **7** shows the main components and areas of KLWT. In order to realize the acoustic testing capability, test section is surrounded by the anechoic room with non-sound-reflective wedges, and corner vanes and motor system are covered with punching metal and glass wool to absorb the sound. Only one operator can control and check the wind tunnel and measurement system online, since measurement sequence basically proceeds automatically, and this feature gives KLWT high productivity of the data.



KLWT has two test section configurations. One of them is closed test section that is mainly for a force measurement, and the other is open test section that is basically for an acoustic testing.





Closed test section

Open test section

Figure 8- Closed and open test sections without model at KLWT

KLWT has two model support systems. One of them is the sting support system that can support the model from backward with sting and change the model attitude (roll, pitch, yaw angles) to the flow and its height. The other is the strut support system with external balance, which can support the model from the ground side and can change model attitude. Figure 9 shows the tests with closed test section using those support systems, and tests with open test sections for acoustic purpose.





Test with the sting support in closed section [13] Test with the strut support in closed section





Acoustic test with half model [14-17]

Acoustic test with rotor model

Figure 9- Closed and open test sections with models at KLWT

# 2.3 Flow quality

Flow quality of KLWT was measured through 1-year flow calibration campaign during 2019-2020. Table **2** and Figure **10** show the result of flow calibration for the test section with 3.0[m] width.

Static pressure gradient	less than ± 0.001 [1/m]	dCp/dx, x:stream wise direction
Flow angularity	less than ± 0.1 [deg]	
Velocity distribution	less than ± 0.3 [%]	Cross section
Temperature distribution	less than ± 1.0 [K]	Cross section
Flow turbulence distribution	less than ± 0.2 [%]	Cross section

Table 2– KLWT Flow Quality (Closed test section with 3.0[m] width)

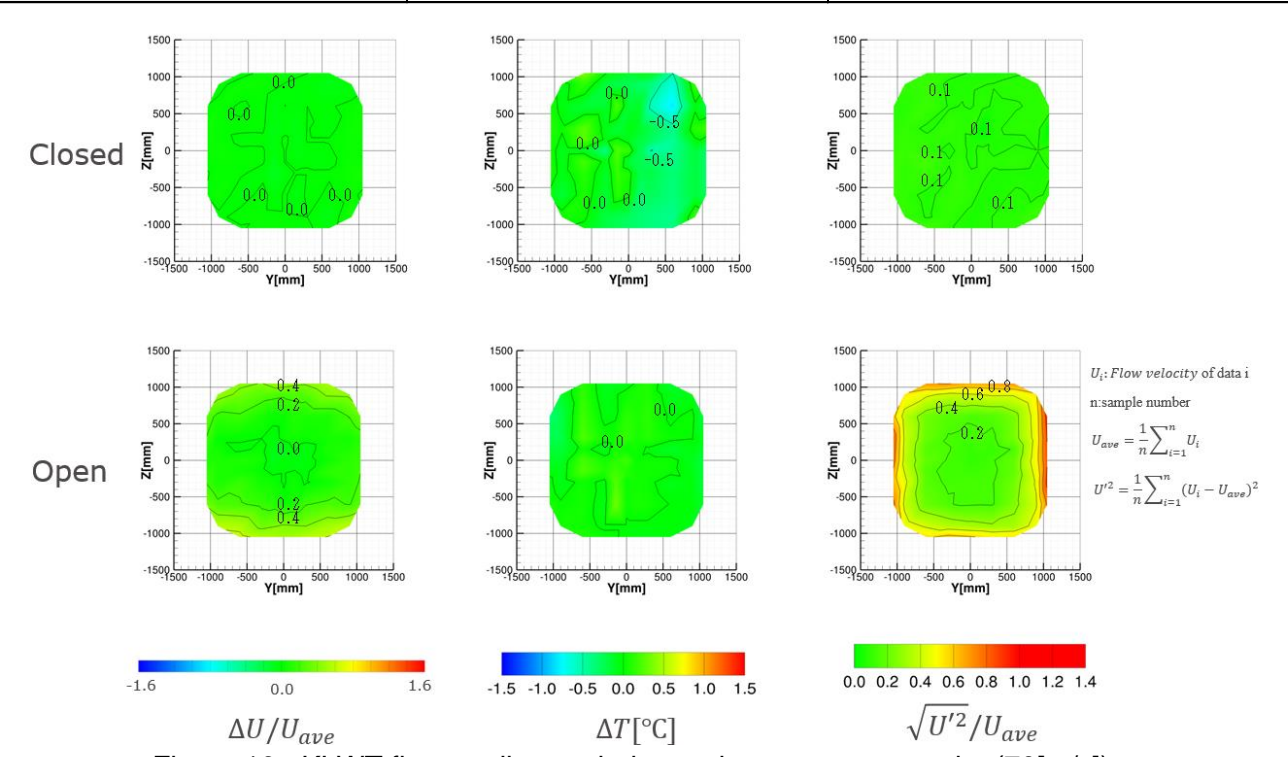


Figure 10– KLWT flow quality at wind tunnel center cross section(70[m/s])

Figure **11** shows the background noise of KLWT with open section(3[m] width). Even at maximum flow speed 85[m/s] noise level is 80[dB(A)] and this value is lower than the typical aircraft noise level.

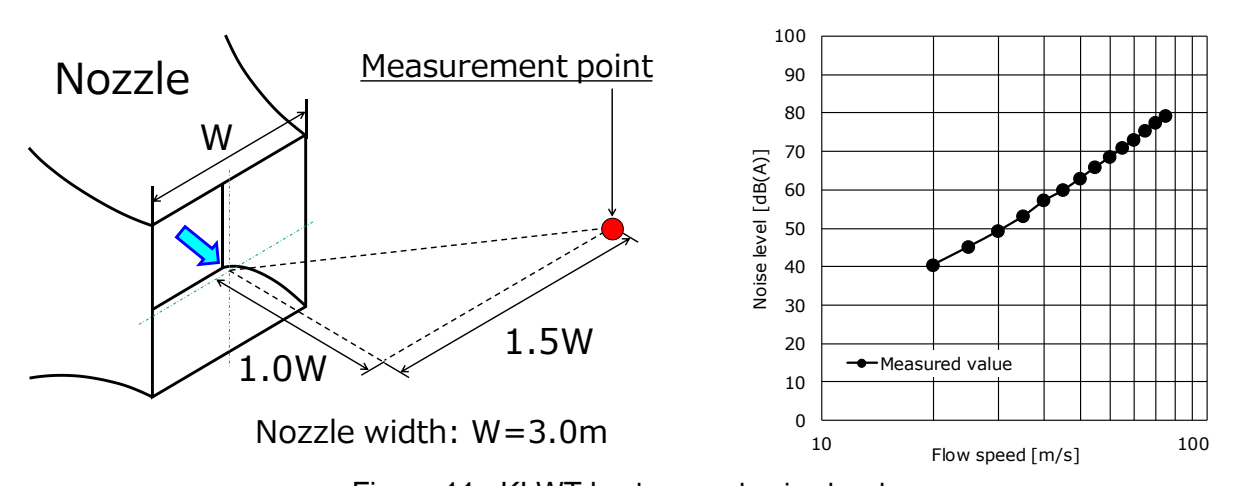


Figure 11- KLWT back ground noise level

# 2.4 Measurement system

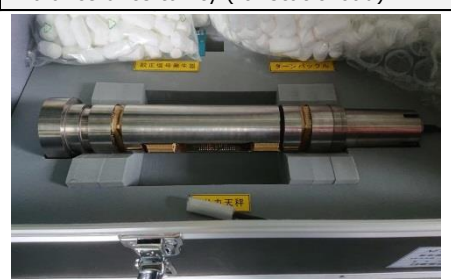
This subsection describes the measurement related things at KLWT.

#### 2.4.1 Force measurement

For the force measurement at KLWT, brand-new force sensors for both the sting support system and the strut support system were developed, since expected model size is larger than the model for old wind tunnel and dynamic pressure is almost 4 times larger than old wind tunnel. Table 3 shows the specifications for those two balances. Especially for the new internal balance, flange was adapted instead of cone as the model/balance interface, to reduce the uncertainty of the model fixation and improve the repeatability of the assembly since there are relatively large space inside the model. Flange interface also made assembly process easier than cone interface. To reduce the uncertainty more severely, ultrasonic bolt axial force gauge was also introduced and used to keep the axial force always constant both at calibration and testing processes. Figure 12 shows these balance and gauge.

Table 3– Specifications of KLWT balances

Items		Balance	for sting support sys	stem	Balance	for strut support sys	tem	
Dalance Tun	Balance Type		Internal Balance			External Balance		
ватапсе тур			Dia =60[mm], Flange Dia =	= 75[mm])	(Plat for	m type)		
Balance Man	ufacturer	NISSHO	ELECTRIC WORKS		HORIBA	Europe GmbH NL Da	rmstadt	
Balance Man	ufacturer Country	JAPAN			GERMAN	Υ		
Balance Mod	Balance Model Number		LMC-61448 HE Project No.21001079			ct No.2100107965		
	Axial force	FX	±1500	[N]	FX	±4000	[N]	
	Side force	FY	±5000	[N]	FY	±4000	[N]	
Full Scale	Normal force	FZ	±10000	[N]	FZ	±12000	[N]	
ruii Scale	Rolling moment	MX	±900	[Nm]	MX	±2000	[Nm]	
	Pitching moment	MY	±1200	[Nm]	MY	±4000	[Nm]	
	Yawing moment	MZ	±800	[Nm]	MZ	±4000	[Nm]	
Balance unce	ertainty (for static load)		2σ less than 0.2%FS			2σ less than 0.25%FS		







Internal balance

Ultrasonic Axial force gauge

External balance

Figure 12- Force measurement devices of KLWT

## 2.4.2 Pressure measurement

For the steady pressure measurement at KLWT, PSI System 8400, which is international standard in the wind tunnel society, is used.



Figure 13– PSI System 8400

## 2.5 Check model

It was necessary for KHI to prepare a brand-new check standard model for KLWT, because of the increase of the model size and dynamic pressure. Firstly, as the shape of this check model, KHI selected NASA Common Research Model (CRM) [10-12] from various public/private shapes shown in Figure 14, considering following objectives to be aimed, after some discussions inside KHI.

- Check model for the checking process of various systems including model support system, measurement system, and wind tunnel control system of KLWT.
- Check model for the new KLWT to insure the data quality (data comparison with other WTs)
- Test bed for various trials (Test technologies, acoustic, aerodynamics) and presentation
- CFD validation (CFD/EFD cooperation)



AGARD-B/C (1952-) ONERA-MX (1969-) DLR-F4/F6(198X-) [18] NASA-CRM (2008-) [12] Figure 14– KLWT Check model candidates (public shapes of check standard model)

The ratio of the check model wing span to wind tunnel width was determined to be equal with that of the original NASA 2.7% model [10] at NTF. And model scale 3.23% was determined by this restriction (From the view point of balancing the requirement for the reduction of wall and boundary layer influence to be received and the increase of Re number to be achieved, this ratio/scale is reasonable). In order to use this model as the system checking processes of both the sting support system and the strut support system, this model was designed to be supported by both support systems.

In order to use this model for the model system endurance check fully, clean wing was insufficient, so it was decided to let the KHI check model have high lift wing in addition to the clean wing.

After here, the check model for KLWT with clean wing (high speed wing) will be expressed as "KHI CRM with High Speed wing (KHI CRM-HS)", and check model with high lift wing will be expressed as "KHI CRM with High Lift wing (KHI CRM-HL)". Since around 2017, CRM-HS shape was only available for KHI, KHI CRM-HS was firstly designed and manufactured by Mar.2019. and used for the first blowing test of KLWT. Table 4 shows the specifications of KLWT check standard model, and Figure 15 shows the photos of KHI-CRM-HS with sting support system and strut support system.

KHI CRM-HS is purely for force measurement check, so it does not have any pressure taps on it.

	KLWT check model information										
Name with wing1		Reference information (full scale)									
Name with wing2	KHI High Lift Common Research Model (KHI CRM-HL)										
Model Type	Full Span Model	Scale	3.23 [%]			100			[%]		
Wings	Wing1:High Speed (HS) Wing2:High Lift (HL)	Reference Area	0.400299	[m²]	620.465	[inch²]	383.690	[m <sup>2</sup> ]	594720	[inch <sup>2</sup> ]	
Supports	Strut Support (with External Balance)	Full Span (No cap included)	1.89804	[m]	74.726	[inch]	58.763	[m]	2313.5	[inch]	
(Balance)	Sting Support (with Internal Balance)	Mean Aerodynamic Chord (MAC)	0.22627	[m]	8.908	[inch]	7.005	[m]	275.8	[inch]	

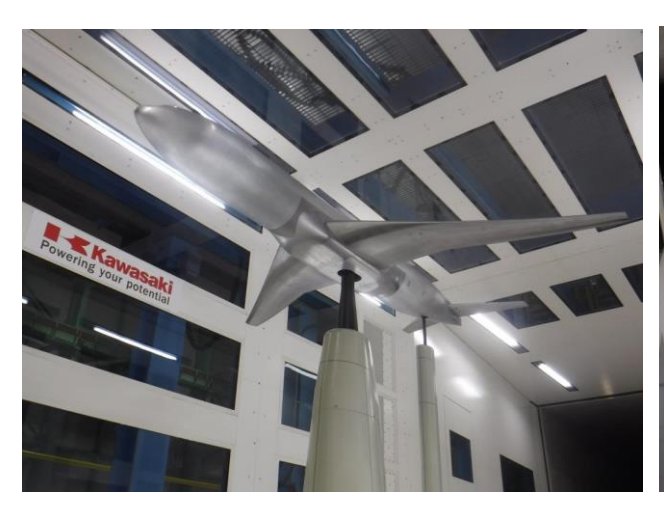
Table 4– KLWT check model specifications

NOTE: Full scale value are based on the Reference [10-12]





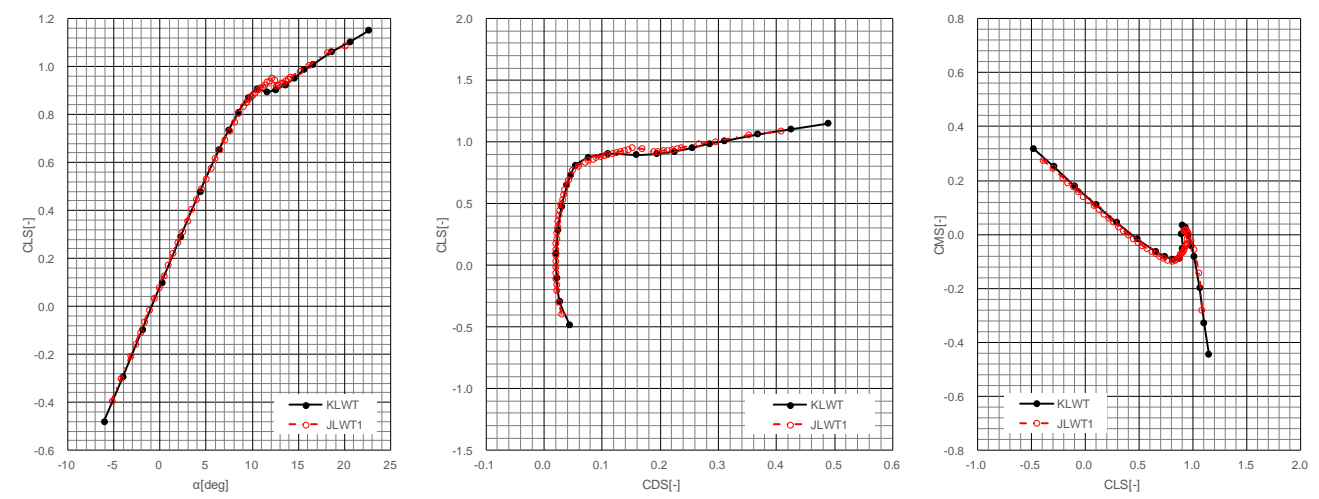
KHI CRM-HS with the sting support system





KHI CRM-HS with the strut support system
Figure 15– KLWT check model (KHI CRM-HS model) in the test section

Figure **16** shows the representative test results of 3.23% KHI CRM-HS compared with the test results of 4.32% JAXA CRM model at JAXA low speed wind tunnel 1 (JLWT1) [19]. Both results are corrected by wall interference, and matching seems reasonably good.



NOTE: KLWT: W3\*H3[m], Closed, U=70[m/s], Rec=1.08[\*10<sup>6</sup>], JLWT1: W5.5\*H6.5[m], Closed, U=60[m/s], Rec=1.09[\*10<sup>6</sup>] Figure 16– KLWT check model (KHI CRM-HS model) test results comparison

## 3. KHI CRM-HL

Preliminary configuration of CRM-HL was firstly developed around 2016-2017[1]. After huge amount of analyses and discussions using data sets of testing campaigns with 10% model at NASA 14by22ft and QinetiQ 5[m] low speed wind tunnel around 2018-2019, "the reference configuration" of CRM-HL finally developed around 2022 by CRM-HL Ecosystem team refining the preliminary shape [1-4,9].

# 3.1 Model specifications

Specifications of KHI CRM-HL was defined in 2017 to 2022 through the discussion inside KHI and dialogue with Ecosystem team. Table **5** shows the final specifications of KHI-CRM-HL.

		iu	310 0	1 (1 11 (	<u> </u>	IL IIIOGCI SPCCIIICG	10110	
Name	KHI CRM-HL				·	Sting	Blade sting	
Shape	CRM-HL reference	e config	guratio	n		Nacelle/Pylon	Yes	On/Off possible
Туре	Full Span Model					Nacelle chine	Yes	On/Off possible
Scale	3.23 [%]					Flap Track Fairing	NASA style	Not hinged version
Supports (Balance)	Sting Support With 10[kN] Internal Balance					Landing Gear	Not applicable	Future plan
	Strut Support With 12[kN] External Balance					Horizontal tail	Yes	On/Off possible
	Config	Symbol	High lift device angle[deg]		gle[deg]	Vertical tail	Not applicable	Future plan
	Config.	Symbol	Slat	Inb'd Flap	Outb'd Flap	Pressure taps	126 taps	119 on wing, 7 on Nacelle
Wing Config.	Take off	то	22	25	25	Maximum Lift	7000 [N]	Expected value
Comigi	Landing	LD1			37	Strength	Safety Margin > 4.0	
	Landing	LD2	30	37	34	WT	KLWT	

Table 5- KHI CRM-HL model specifications

# 3.2 Model Shape definition

For the outer shape of the KHI CRM-HL model, "The reference configuration" of CRM-HL provided by the Ecosystem team was used. Especially CAD model with 0.2" thickness trailing edge was used. Table 6 shows the CAD files that was used for KHI CRM-HL. Regarding the missing information such as Flap Track Fairings (FTF) and slat tracks shapes, those shapes prepared for the NASA 5.2% CRM-HL model were provided from NASA team and used for KHI CRM-HL.

		Table	e 6– CAD files used for i	ATI CRIVI-TIL			
				Reference Configuration			
No.	Class1	Class2	CAD fil	e name	Received date/source		
			Inboard	Outboard	date	source	
1		WRP definition	wingfeaturestokhi.stp		2020/10/16	Web	
2	ALL	Pressure sections	wingfeaturestokhi.stp		2020/10/16	Web	
3		Axis	axis.stp	axis.stp			
4	Fuselage	Fuselage Surface	HLPW-4_CRM-HL_40-37_Nomin	2020/10/14	Web		
5		Main Wing Surface	wing01.stp	2022/1/20	Web		
6	Main Wing	Main Wing Strake	strk01.stp		2022/1/20	Web	
7	Main wing	WUSS	wuss01r1.stp	wuss02r1.stp	2022/3/10	Web	
8		COVE	fcove01r1.stp	fcove02r1.stp	2022/3/10	Web	
9		Slat wing component	slat01r1.stp	slat02r1.stp	2022/3/10	Web	
10	Slat	Slat Support	1299781_crm_5-2p_assy_REV-	\.stp	2022/3/21	NASA	
11		Slat Rotation Definition	1299781_crm_5-2p_assy_REV-	1299781_crm_5-2p_assy_REV-A.stp			
12		Flap wing component	flap01r1.stp	flap02r1.stp	2022/3/10	Web	
13	Flap	Flap Support	No-Brakcet	No-Brakcet	-	-	
14	гіар	Flap Rotation Definition	fpos01refldg-25.stp、-37.stp、-40.stp	fpos02refldg-25.stp、-34.stp、-37.stp	2022/3/10	Web	
15		FTF	1299781_crm_5-2p_assy_REV-	1299781_crm_5-2p_assy_REV-A.stp			
16	Dower plant	Pylon	pyln01.stp		2022/1/20	Web	
17	Power plant	Nacelle	nacl01.stp		2022/1/20	Web	

Table 6- CAD files used for KHI CRM-HL

# 3.3 Pressure taps

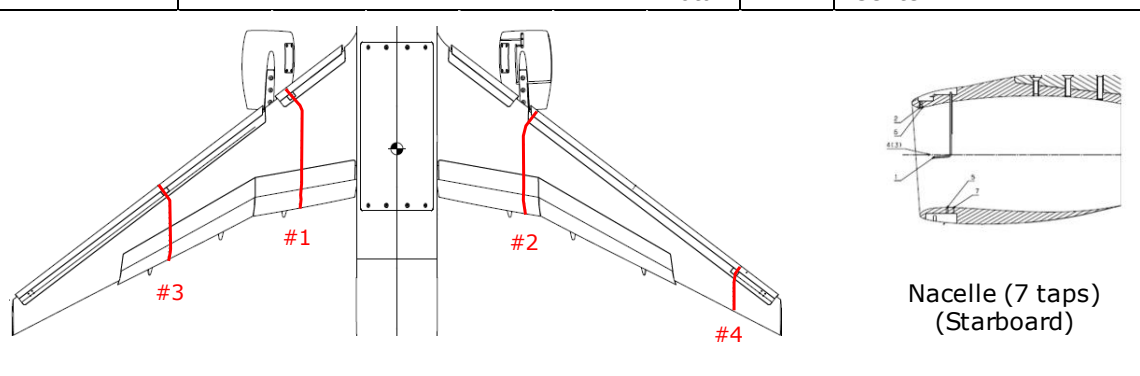
For KHI CRM-HL, pressure taps were necessary to confirm the pressure measurement system of KLWT. Total 126 pressure taps were distributed only on the wing and nacelle of KHI CRM-HL. On the wing, 119 static pressure taps were distributed in 4 stations as shown in Table **7** and Figure 17 to capture the phenomena such as flow separations behind the nacelle/pylon and outer wing, which are important for the CFD validation. Locations of these pressure taps and stations were extracted from NASA 5.2% CRM-HL model that have 10 stations in order to keep the comparability. On the nacelle, 6 static pressure taps and 1 total pressure tap are distributed as shown in Table **8** and Figure 17. Table **9** gives more detail information on pressure taps of KHI CRM-HL. No Kulite or equivalent pressure sensor for unsteady measurement was prepared for the KHI CRM-HL model.

Table 7– KHI CRM-HL pressure taps on wing

						•	•	
Component	Station		η <sup>*2</sup>	Static pressure taps			ps	Note
Component	KHI	NASA*1	η	Slat	Wing	Flap	Total	Note
	#1	2	0.250	5	23	8	36	
	#2	3	0.332	6	15	8	29	*1:Correspondent Station number of
Wing	#3	6	0.594	6	19	8		the NASA 5.2% CRM-HL
	#4	9	0.878	5	16	0	21	*2: η is semi-span ratio
			Total	22	73	24	119	

Table 8– KHI CRM-HL pressure taps on nacelle

			_				
Component		Тор	Port	Starboard	Bottom	Total	Note
	Inner throat	2	1	1	2	6	
Nacelle	Total pressure	-	-	-	-	1	Center
					Total	7	Center



Wing(119 taps)

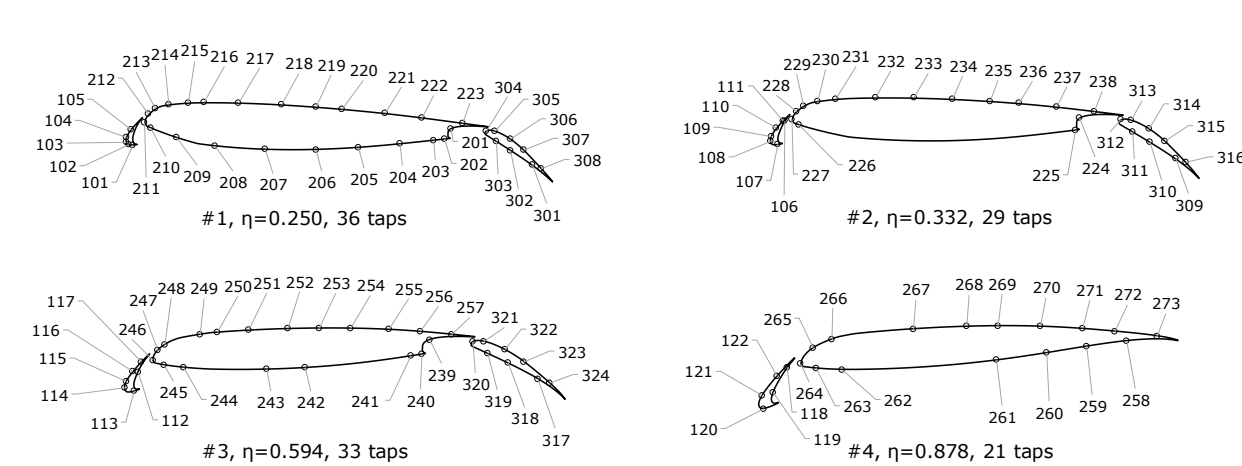


Figure 17– Pressure taps locations of KHI CRM-HL model

Table 9- KHI CRM-HL pressure taps on wing/nacell (detail)

			rab	ie 9– i	KHI C	KIVI-H	L press
Section/η*1	Component	UPR/LWR	STA	BL	WL	No.	Position[%CS]*2
			939.44	-272.90	141.22	101	0.069
			936.73	-274.94	141.48	102	0.060
	Slat	UPR	934.75	-276.23	143.60	103	0.053
			934.90	-275.74	146.89	104	0.053
			937.87	-272.89	152.27	105	0.063
			1161.52	-237.44	150.03	201	0.806
			1157.45	-238.10	142.48	202	0.792
			1149.69	-238.18	141.58	203	0.766
			1126.24	-238.41	138.95	204	0.689
		LWR	1096.88	-238.64	136.27	205	0.591
			1067.44	-238.78	134.74	206	0.493
			1032.07	-238.77	134.84	207	0.376
			996.79	-238.54	137.43	208	0.259
			970.09	-248.82	144.46	209	0.170
			951.93	-261.92	152.80	210	0.110
	Main		947.51	-264.90	157.17	211	0.095
	wing		950.40	-262.18	163.05	212	0.105
#1			955.15	-258.23	166.85	213	0.121
η=0.250			964.23	-251.12	169.12	214	0.151
			978.36	-240.33	169.51	215	0.198
			988.93	-235.75	169.40	216	0.233
		UPR	1013.15	-235.77	169.13	217	0.313
			1043.40	-235.89	167.76	218	0.414
			1067.55	-236.04	166.05	219	0.494
			1085.65	-236.18	164.46	220	0.554
			1115.77	-236.45	161.35	221	0.654
			1141.38	-236.73	158.14	222	0.739
			1169.79	-237.08	154.15	223	0.833
			1218.80	-242.67	123.61	301	0.996
		LWR	1203.70	-239.98	134.11	302	0.946
			1193.43	-238.25	140.81	303	0.912
	Inb'd		1186.42	-236.36	148.42	304	0.888
	Flap		1192.45	-236.49	148.23	305	0.908
	·	UPR	1203.25	-238.01	142.47	306	0.944
			1212.63	-240.00	134.62	307	0.975
			1225.07	-243.33	121.23	308	1.017
		LWR	1000.43	343.66	163.76	106	0.088
		LVVIX	996.39	348.06	149.53		
			991.96	351.23	151.59	107	0.072
	Slat	UPR				108	
		UFK	992.44	350.59	154.69	109	0.057
			995.58	347.73	159.65	110	0.069
			999.38	344.46	163.85	111	0.084
			1175.58	314.54	163.08	224	0.773
		LWR	1173.28	315.19	155.63	225	0.764
			1008.91	337.46	160.91	226	0.121
			1004.85	340.26	164.28	227	0.105
			1007.51	337.80	169.23	228	0.116
			1011.87	334.19	172.44	229	0.133
	Main		1020.23	327.63	174.79	230	0.165
	Main wing		1030.81	319.51	175.39	231	0.207
#2 η=0.332	, <b>,,</b> ,,,,	UPR	1054.65	313.42	175.81	232	0.300
11-0.552		UPK	1077.32	313.43	175.69	233	0.389
			1099.96	313.50	174.90	234	0.477
			1122.60	313.62	173.58	235	0.566
			1139.55	313.73	172.26	236	0.632
			1162.11	313.93	170.03	237	0.720
			1184.61	314.17	167.28	238	0.808
			1232.68	319.60	137.94	309	0.996
		LWR	1217.51	316.97	148.12	310	0.937
		LVVIX	1207.19	315.30	154.57	311	0.937
	Teals I al						
	Inb'd Flan		1200.20	313.46	161.97	312	0.869
	Flap	LIDE	1206.19	313.58	161.85	313	0.892
		UPR	1217.06	315.03	156.40	314	0.935
			1226.46	316.97	148.75	315	0.972

e taps		_					
Section/η*1	Component		STA	BL	WL	No.	Position[%CS]*2
		LWR	1182.28	-587.99	179.05	112	0.080
			1180.61	-590.04	170.68	113	0.071
	Clat		1176.72	-592.84	172.27	114	0.049
	Slat	UPR	1177.32	-592.14	175.01	115	0.053
			1180.22	-589.53	179.42	116	0.068
			1183.57	-586.62	183.28	117	0.087
			1305.77	-563.25	191.26	239	0.757
			1302.67	-563.81	184.87	240	0.740
			1297.89	-563.88	184.09	241	0.714
		LWR	1253.08	-564.34	178.90	242	0.714
		LWIX	-				
			1236.99	-564.40	178.20	243	0.380
			1201.74	-573.08	179.80	244	0.186
			1193.20	-579.42	181.51	245	0.140
			1188.66	-582.68	183.84	246	0.115
	Main		1190.57	-580.87	187.95	247	0.125
	wing		1193.57	-578.37	190.33	248	0.142
#3 n=0.594	9		1208.74	-566.51	193.96	249	0.225
., 0.55			1216.00	-562.96	194.57	250	0.265
		LIDD	1229.21	-562.89	195.47	251	0.337
		UPR	1245.74	-562.83	196.16	252	0.428
			1258.96	-562.81	196.40	253	0.500
			1272.22	-562.81	196.36	254	0.573
			1288.75	-562.85	195.83	255	0.664
			1301.96	-562.93	194.93		
						256	0.736
			1315.13	-563.04	193.68	257	0.808
		LWR	1351.73	-567.76	174.17	317	1.009
			1339.06	-565.79	181.04	318	0.939
			1330.38	-564.67	185.24	319	0.892
	Outb'd		1324.16	-562.98	190.24	320	0.858
	Flap		1328.85	-562.50	190.40	321	0.884
		UPR	1337.78	-563.33	186.79	322	0.932
		UPK	1345.80	-564.96	181.57	323	0.976
			1356.63	-568.13	172.39	324	1.036
			1384.04	847.65	205.18	118	0.094
		LWR	1380.20	851.20	198.41	119	0.061
	Slat	at UPR	1377.67	853.53	193.92	120	0.039
	o.ac		1377.18	853.57	197.54	121	0.035
			1381.29	849.95	202.90		
						122	0.070
			1475.79	833.25	211.54	258	0.883
			1464.93	833.39	209.98	259	0.789
		LWR	1454.12	833.55	208.14	260	0.696
			1440.57	833.73	206.06	261	0.580
			1398.78	836.54	203.60	262	0.221
#4 η=0.878			1391.83	841.76	204.43	263	0.161
., .0.070			1387.64	844.81	206.05	264	0.125
	Main		1390.90	841.96	210.24	265	0.153
	wing		1396.04	837.86	212.43	266	0.197
			1418.10	832.96	214.89	267	0.387
			1432.41	832.90	215.59	268	0.510
		UPR	1441.00	832.88	215.76	269	0.584
			1452.47				0.584
				832.90	215.60	270	
			1463.91	832.95	214.96	271	0.781
			1472.47	833.02	214.22	272	0.854
	-	<u> </u>	1483.86	833.13	212.90	273	0.952
Component		ition	STA	BL	WL	No.	Note
	Center	-	814.64	316.30	77.87	501	Total pressure
		Тор	803.08	310.86	124.39	502	-
	Throat	Port	811.89	268.54	75.45	503	-
Nacelle	IIIIUdL	Starboard	808.59	363.17	85.70	504	-
		Bottom	826.21	321.75	31.35	505	-
	NASA	Тор	805.45	310.93	124.50	506	-
	Throat	Bottom	832.31	321.99	31.10	507	-
		2000111			0	- **	
_	_	_	_	_		_	_
-	-	-	-	-	-	-	-
-	-	wing a	-	-	-	-	-

<sup>\*1:</sup>  $\eta$  semi-span ratio, \*2:CS is the local chord length of the stowed (clean) wing at each section.

# 3.4 Model design and fabrication

KHI CRM-HL was designed by KHI from 2017 to 2022, especially in between Jan. to Jul.2022, detail design was done using the provided reference shapes according to the guideline [2] of CRM-HL Ecosystem with full support of the Ecosystem team. For example, pressure tubes for slat surface are routed in the slat truck to avoid any additional aerodynamic interference that does not exist in the real flight. Considering the financial limitations for this model, only forward fuselage frame structure and wing with high lift devices were newly designed and manufactured i.e. blade sting and mid and after fuselage parts are shared by both KHI CRM-HS and KHI CRM-HL model as shown in Figure 18. (Some of the existing parts for KHI CRM-HS were used for KHI CRM-HL.) Figure 19 shows the model design results of KHI CRM-HL. This model can be supported by both the sting support system and the strut support system. Before proceeding to the fabrication, CAD model for the KHI CRM-HL was finally compared with the "Bare cad model" for the future workshop (HLPW5) as shown in Figure 20, and no difference was found between two cad models. After this confirmation, KHI fabricated the 3.23% KHI CRM-HL model from Jul.2022 to Dec.2022.

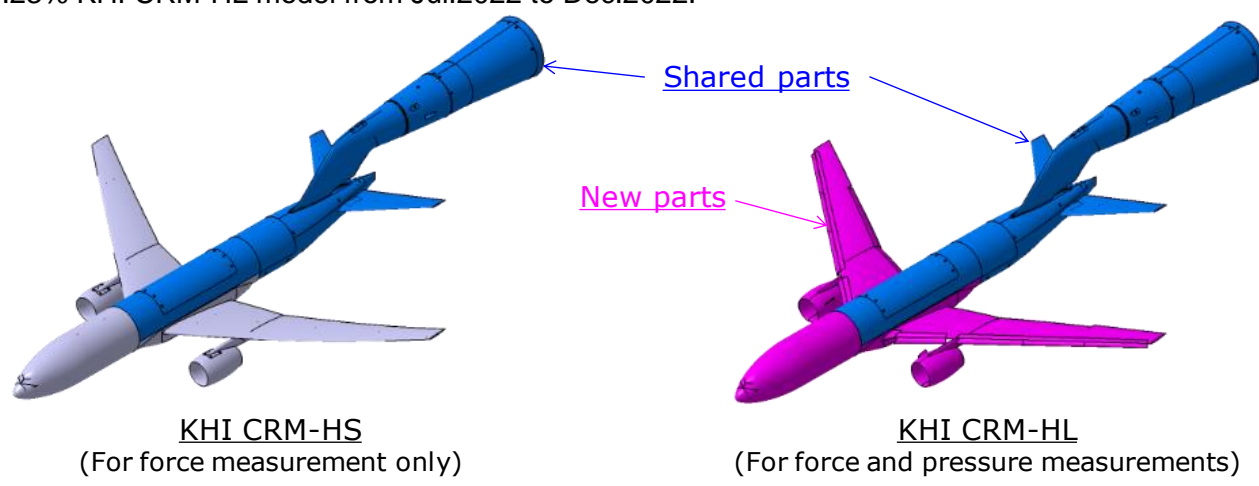


Figure 18– Shared parts of the KHI CRM-HS and the KHI-CRM-HL model

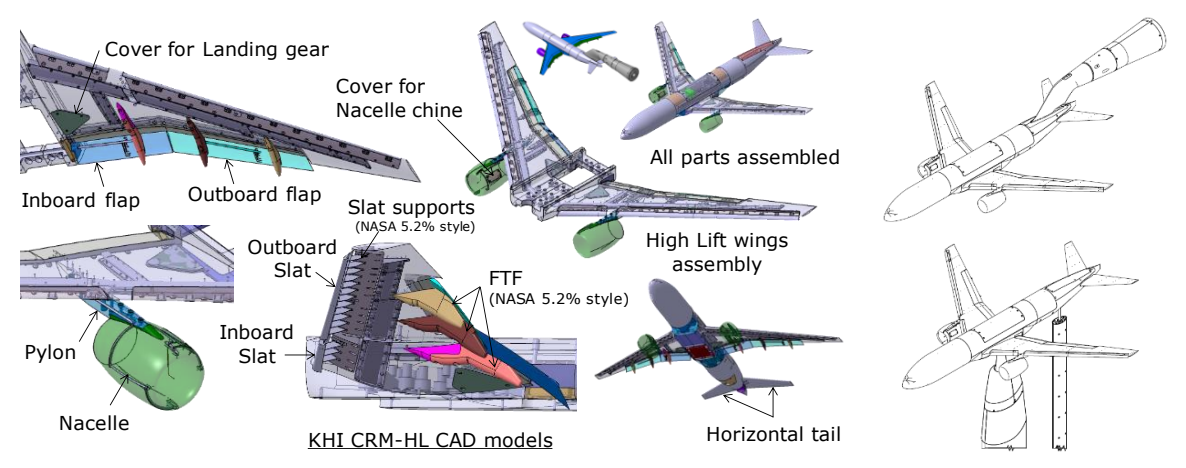


Figure 19- KHI-CRM-HL model design results

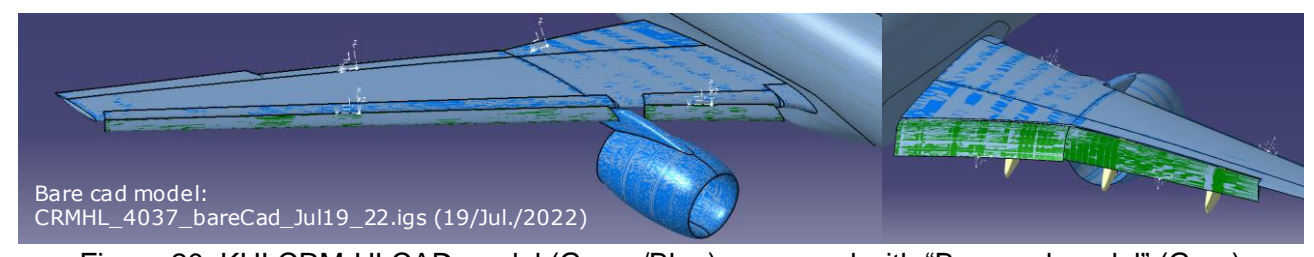


Figure 20–KHI CRM-HLCAD model (Green/Blue) compared with "Bare cad model" (Gray)

# 4. Testing

This section describes the testing campaigns with KHI CRM-HL at KLWT

# 4.1 Test overview

So far, two testing campaigns with KHI CRM-HL at KLWT were done as shown in Table 10.

In the first testing campaign in Oct. 2022, all systems in KLWT were checked with this KHI CRM-HL model prior to the formal data acquisition. In the second testing campaign from Dec. 2022 to Jan. 2023, formal data was acquired with the participation of Ecosystem members.

Through both testing campaigns, closed test section with 3[m] nozzle and W3 by H3[m] configuration was selected and used considering the flow quality and future plan of KLWT, and the wind tunnel model was mounted on the sting support system using blade sting\*1 and the internal balance.

Due to the time restriction, only the reference landing configuration was tested in the 2<sup>nd</sup> testing. \*1: Blade sting outer shape is based on that of the sting for the original 2.7% NASA CRM (-HS) model.

Table 10- Summary of KHI CRM-HL testing campaigns

Items		1 <sup>st</sup> testing campaign	2 <sup>nd</sup> Testing campaign
Test purpose		Preliminary system check	Formal data acquisition
Test Identification	n Number in KHI	A61W	A64W
	Preparation	17 <sup>th</sup> Oct. to 26 <sup>th</sup> Oct.2022	19 <sup>th</sup> Dec.2022 to 6 <sup>th</sup> Jan.2023
Test period	Wind-on test	26 <sup>th</sup> Oct. to 31 <sup>st</sup> Oct.2022	6 <sup>th</sup> Jan. to 17 <sup>th</sup> Jan.2023
	Note	11 working days	16 working days
Wind tunnel	Name	KLWT	KLWT
wind tunner	Nozzle	3.0 [m] nozzle	3.0 [m] nozzle
Tost section	Туре	Closed	Closed
Test section	Size	W3.0 by H 3.0 [m]	W3.0 by H 3.0 [m]
Model support sys	tem	The sting support system	The sting support system
Force sensor		Internal Balance	Internal Balance
Sting		Blade sting	Blade sting
	Name	KHI CRM-HL	KHI CRM-HL
Model	Туре	Full span model	Full span model
Model	Configuration	LD1,LD2	LD1
	Note	(without chine/pressure port)	-
		Force and moment	Force and moment
Measurements		Angle of attack (AOA)	Angle of attack (AOA)
Measurements		-	Surface pressure
		-	Visualization (Oil flow/tuft)
	Flow speed	20 - 90 [m/s]	34 to 85 [m/s]
	Mach	0.06 to 0.27 [-]	0.10 to 0.25 [-]
Test condition	Emvironmental pressure	Ambient	Ambient
	Angle of attack	-10 to 24[deg]	-10 to 20[deg]
	Angle of sideslip	0[deg]	0[deg]
Ecosystem team p	participation	-	6 <sup>th</sup> Jan. to 13 <sup>th</sup> Jan.2023

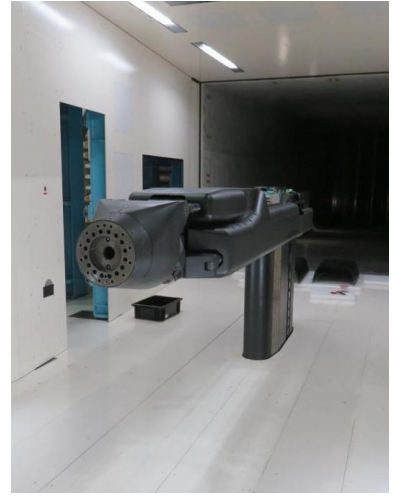
# 4.2 1st testing campaign

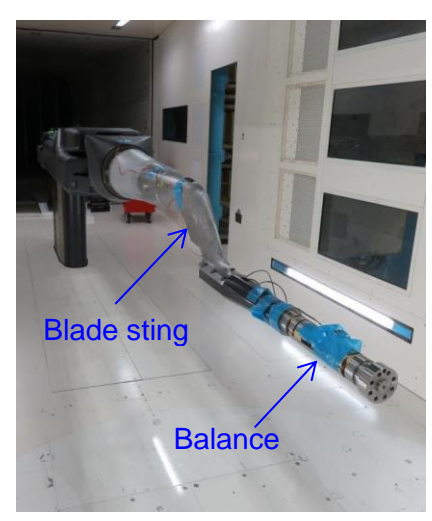
1<sup>st</sup> testing campaign of KHI CRM-HL at KLWT was done in Oct.2022. As mentioned in the 2.5, KHI CRM-HL model was prepared to check the systems of KLWT, and this test was the first high-loading testing for KLWT, so some of system check was done in the testing.

Firstly, the blade sting was confirmed to be able to endure static load that is as same as the expected air load in the wind on condition using dead weights before installation as shown in Figure 21(left).

After the sting endurance confirmation, the blade sting and the internal balance were installed onto the sting support system in the closed test section of KLWT as shown in Figure 21(mid and right). And then, KHI CRM-HL model was installed onto the balance using ultrasonic axial force gauge. Table 11 shows the configurations of KHI CRM-HL model in the 1st testing campaign. As shown in the table, Nacelle chine and pressure ports were not in time for this testing.







Loading check

Sting support system

Balance installed on the sting

Figure 21– Preparation process of 1st testing campaign of KHI CRM-HL

Table 11– Model configurations of in the 1<sup>st</sup> testing campaign

		Name	KHI CRM-HL	Flap Track Fairing	NASA style (not hinged ver.)
Model		Shape	CRM-HL reference configuration	Nacelle/Pylon	On
		Scale	3.23 [%]	Nacelle chine	Not applicable (not in time)
	LD1	Slat	30 [deg]	Landing Gear	Not applicable
		Inboard flap	40 [deg]	Horizontal tail	On/Off
Wing		Outboard flap	37 [deg]	Vertical tail	Not applicable
vvilig		Slat	30 [deg]	Pressure taps	Not applicable (not in time)
	LD2	Inboard flap	37 [deg]	Gap seal (flaps)	On
		Outboard flap	34 [deg]	Transition trips	On

The wind-on testing started with slow velocity (20 [m/s]) very carefully and finished with the velocity up to 90 [m/s] confirming and monitoring the vibration of wind tunnel, test section and KHI CRM-HL model. In this process, some minor system troubles happened but those were fixed soon firmly. Through these check runs, KLWT systems including Wind Tunnel flow driving system, Model support system, and Measurement system were confirmed to be able to endure the wind-on testing with KHI CRM-HL model under high load condition. Table **12** shows the test condition in the system checking process, and Figure **22** shows the KHI CRM-HL model in the 1<sup>st</sup> testing campaign.

Table 12– Test conditions for the wind-on system endurance check in the 1<sup>st</sup> testing campaign

Diverse	Date	Run#	V	Mach	AOA	\//in =	HT	Flap GAP	Puressure	Judge	Information
Purpose	Date	Rull#	[m/s]	[-]	[deg]	Wing	п	Sealing	tap plug	Juuge	Information
		A61W001	20	0.06	-10~24					NG	SYS error
	26-Oct-22	A61W002	20	0.06	-10~24			QinetiQ	No -	NG	SYS error
		A61W003	20	0.06	-10~24					OK	
		A61W004	20	0.06	-10~24					OK	Repeatability
		A61W005	40	0.12	-10~24	LD1	ON			OK	
System		A61W006	50	0.15	-10~24					OK	
confirmation		A61W007	60	0.18	-10~20					NG	setting error
	27-Oct-22	A61W008	60	0.18	-10~20					OK	
		A61W009	68	0.20	-10~20					OK	
		A61W010	80	0.24	-10~20					OK	
		A61W011	90	0.27	-10~20					NG	setting error
		A61W012	90	0.27	-10~20					ОК	stopped at 19 deg



Figure 22– KHI-CRM-HL model at KLWT in 1st testing campaign (Oct.2022)

After the wind-on system endurance check, some measurement trial runs were done also as shown in the Table **13**. In the trial, only force data was acquired and confirmed to have reasonable repeatability and reasonably small hysteresis. Test data acquired in this trial is not shown in this paper, since the model was not perfect condition and it might be confusing for the reader. (Model was without chine, pressure taps and surface treatment, so the data got in this trial was not formal).

Table 13– Test conditions for the measurement trial in the 1st testing campaign

Purpose	Date	Run#	V	Mach	AOA	Wing	HT	Flap GAP	Pressure	Judge	Information
ruipose	Date	Kull#	[m/s]	[-]	[deg]	wilig		Sealing	tap plug	Judge	Illomiation
	27-Oct-22	A61W013			-10~20					OK	
		A61W014			-10~20			ONERA		OK	
		A61W015			-10~20		ON			OK	Repeatability
		A61W016			-10~20		No			OK	Repeatability
		AOIWOIO			20~-10	LD1				OK	Repeatability & hysteresis check
		A61W017		0.20	-10~20					OK	
Aerodynamic	28-Oct-22	A61W018			-10~20					OK	Repeatability
data		A61W019	68		-10~20				Plugged	OK	Repeatability
measurement trial					20~-10				riuggeu	OK	Repeatability & hysteresis check
Cital		A61W020			-10~20					OK	stopped at 14 deg (Sys error)
		A61W021			-10~20					OK	
		A61W022			-10~20					OK	Repeatability
		A61WU22			20~-10	LD2				OK	Repeatability & hysteresis check
		A61W023			-10~20					OK	
	31-Oct-22	A61W024			-10~20		ON			OK	Repeatability
		A01W024			20~-10					OK	Repeatability & hysteresis check

# 4.3 2<sup>nd</sup> testing campaign

After the 1<sup>st</sup> testing, nacelle chines for the KHI CRM-HL were designed and manufactured using the CAD file provided by Ecosystem team as shown in the Figure 23. Simultaneously, surface treatment of the main wing was also done in order to prevent the rust and to enhance the visualization, and then pressure taps and tubes were also added for the steady pressure measurement. The fabrication and inspection of the KHI CRM-HL were completed on mid of Dec.2022 as shown in Figure 24.

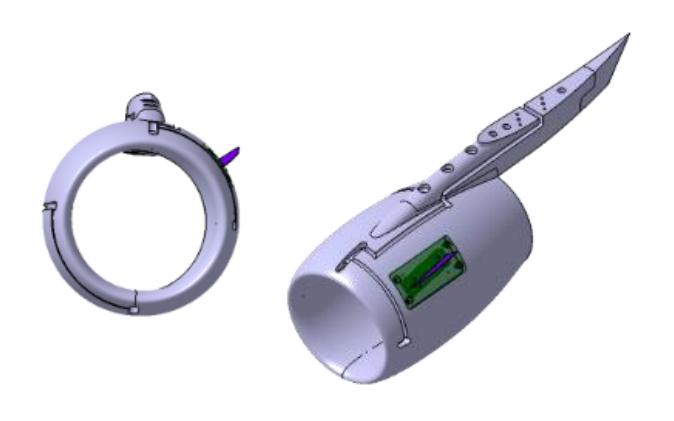




Figure 23- Nacelle chine design and manufacturing results



Figure 24– KHI-CRM-HL model manufacturing results in Dec.2022

After the completion of model fabrication, 2<sup>nd</sup> testing campaign started on 19<sup>th</sup> Dec. 2022 and finished on 17<sup>th</sup> Jan.2023. Table **14** shows the configurations of KHI CRM-HL in the 2<sup>nd</sup> testing campaign. In this 2<sup>nd</sup> testing, only one configuration LD1(the reference landing configuration) was tested due to the time constrain.

Table 14– Configurations of KHI CRM-HL in the 2<sup>nd</sup> testing campaign

					g •ap ag		
		Name	KHI CRM-HL	Flap Track Fairing	NASA style (not hinged ver.)		
Model		Shape	CRM-HL reference configuration	Nacelle/Pylon	On		
		Scale	3.23 [%]	Nacelle chine	Yes (On/Off)		
		Slat	30 [deg]	Landing Gear	Not applicable		
	LD1	Inboard flap	40 [deg]	Horizontal tail	On/Off		
Win =		Outboard flap	37 [deg]	Vertical tail	Not applicable		
Wing		Slat		Pressure taps	126		
	LD2	Inboard flap	Not applicable (Not tested)	Gap seal (flaps)	On		
		Outboard flap	,	Transition trips	On/Off		

## 4.3.1 Measurement

In the 2<sup>nd</sup> testing campaign, following data sets were measured/acquired by the measurement system. All measurements were steady one (not unsteady) except the model acceleration for monitoring.

- · Aerodynamic load (6 components force and moment) onto the model
- · Angle of attack (AOA) of the model
- Surface static/total pressure of the model wing and nacelle
- Model Acceleration (for the vibration monitoring purpose)

Figure 25 shows the wiring diagram of the measurement system used for those measurements. Only atmospheric pressure sensor was set outside the model and other sensors were installed in the model. For the analogue output sensors, signal conditioners (Low-path filters) were set and used between amplifier and the analog/digital (A/D) converter in order to damp the noisy high frequency component of the signal. After signal conditioning, analogue signals were digitized by the A/D converter. All devices such as amplifiers, filters, etc. except sensors and Scanner digitizer interface (SDI) for scanners were set in the air-conditioned room for the stable behaver.

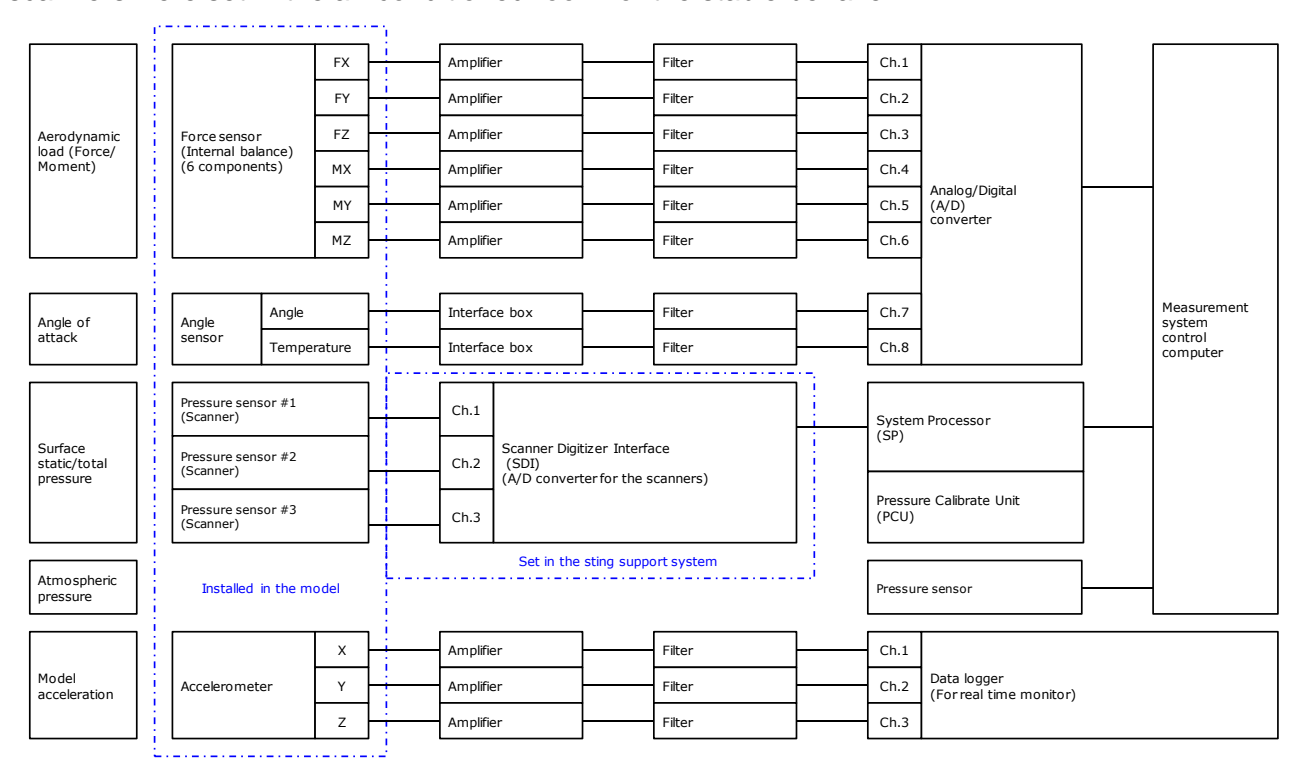


Figure 25– Wiring(connection) diagram of the measurement system in the 2<sup>nd</sup> testing campaign

Table **15** shows the setting information of the Low-path filter and A/D converter for the force, angle, pressure and acceleration sensors. These settings are based on the experiences of KHI wind tunnel team and now typical at KLWT.

	Table	10 Mcasarch	icht settings	11 1110 2 1031	ing campaign	
	Signal conditione	r(Low-path filter)	Ana	log/Digital(A/D) conve		
Sensors	Туре	Cutoff frequency	Sampling rate	Sampling time	Sampling points	Note
	[-]	[Hz]	[Hz]	[sec]	[sec]	
Force sensor	Bessel	10	100	2.0	200	for steady measurement
Angle sensor	Bessel	10	100	2.0	200	for steady measurement
Pressure scanner	-	-	100	2.0	200	for steady measurement
Accelero meter	Bessel	500	1000	-	-	for vibration monitoring

Table **16** shows the measurement devices, parts, and materials used for the 2<sup>nd</sup> testing campaign, Basically, all sensors and devices used for the testing has traceability up to the national or international measurement standard directly or indirectly for the data quality assurance.

Table 16– Measurement related items in the 2<sup>nd</sup> testing campaign

Purpose	Items	Product/Model number	Quantity	Label		Manufacturer/NOTE
	Sensor	LMC-61448 (Internal Balance)	1	-	S/N:0001	NISSHO ELECTRIC WORKS/ Inside fuselage
				FX	520836	
				FY	520838	
				FZ	520840	
	Amplifier	SA-570ST	6	MX	520844	TEAC Corporation
				MY	520846	
				MZ	520847	
Aerodynamic load				FX	807837	
(force/moment)				FY	807838	
measurement	0: 10 1::			FZ	807839	NE O
	Signal Conditioner (Low-path Filter)	As-305 (MAINFRAME NF7295)	6		807840	NF Corporation/ (Type:Bessel,48dB/oct)
	(	(,		MX		( , , p = , = , , , , , = = , , , , ,
				MY	807841	
		NIT O D D D	_	MZ	807842	
	A/D converter	NI 9220	1	-	30401607	NI(National Instruments corporation)
	Ultrasonic axial force gauge	MAX II J	1	-	70240	DAKOTA JAPAN (DAKOTA Ultrasonics)
	Torque wrench	QL140N	1	-	200647J	Tonichi Manufacturing Co., Ltd.
Angle of attack	Sensor	QA-2000-010 (Q-Flex) (servo accelerometer)	1	-	SENSOR S/N:A8AG3VB T/A S/N:4003	Honeywell/ Inside fuselage
(AOA)	Signal Conditioner	As-305		Angle	807843	NF Corporation/
measurement	(Low-path Filter)	(MAINFRAME NF7295)	2	Temperature	807844	(Type:Bessel,48dB/oct)
	A/D converter	NI 9220	1	-	30401533	NI(National Instruments corporation)
		ESP-64HD		#1	64639	The Disease of Cushama
	Sensor	(Range:15 [psid])	3	#2	643200	The Pressure Systems Incorporated (PSI)/
	(Scanner)	(Digital Thermal Compensated(DTC))		#3	643201	Inside fuselage
	Scanner Digitizer Interface (SDI)	8411	1	-	S/N:0156	
Surface	Pressure Calibrate Unit(PCU)	8432	1	-	S/N:1797	The Pressure Systems
static/total pressure	System Processor(SP)	8400	1	_	S/N:717	Incorporated (PSI)
measurement	.,	55M700	5	-	-	Scanivalve Corporation/
	Connector	55F700	5	_	-	55 tubes connectable, Inside fuselage
	Tube	UF-M016-100	1	-	-	Junkosya Inc. Polyurethane Tubing Outer Diameter 1.6[mm] Inner Diameter 0.8[mm]
Atmospheric pressure measurement	Sensor	PACE1001 (Range:75-115[kPa]) (Type:IRS0-B) (Precision Pressure Indicator)	1	-	10993223	Druck Ltd./ Back puressure for the PSI scanners
	Sensor	MODEL 65-10 (triaxial) (ISOTRON accelerometer) (Piezoresistive accelerometer) (Voltage output type with pre-amplifier)	1	-	SN13503	Endevco, MEGGITT/ Inside fuselage Document Number X:49140,Y:49430,Z:49140
	Amplifier	AG3103		Х	0300514	
Acceleration	(Line-drive constant-current power	(Charge amplifiler) (Electric Charge/Vlotage input	3	Υ	0300515	A&D Company, Ltd. (NEC Avio)
measurement (for monitoring)	supplier)	switchable)(Power supply for sensor 2[mA])		Z	0300516	()
(101 monitoring)				Х	807843	
	Signal Conditioner (Low-path Filter)	As-305 (MAINFRAME NF7295)	3	Υ	807844	NF Corporation/ (Type:Bessel,48dB/oct)
	(LOW-patri i liter)	(1:1011N1 10011L N1 /293)		Z	807845	(1) pe. bessel, +oub/oct/
	Data logger	RA2300A	1	-	1500146	A&D Company, Ltd.
Computer	Computer	EliteDesk 800 G3	1	-	-	HP
•	Sensor	AC151	1	-	6417	OBISHI Keiki Seisakusho Co.,Ltd.
Level	3611501	ACIJI				

# 4.3.2 Model preparation

As the preparation for the 2<sup>nd</sup> testing campaign, the blade sting was installed on the sting support system in the closed test section, and then the KHI CRM-HL model was set on the sting using internal balance in 19<sup>th</sup> Dec.2022 to 6<sup>th</sup> Jan.2023. AOA sensor, pressure scanners and accelerometer were installed inside the model in this process. More detail information on model will be given in this section.

# (A) Boundary layer transition

In order to reduce the uncertainty due to the boundary layer on the various elements of the high-lift configuration during the wind tunnel testing, boundary layer was artificially tripped using so-called "CAD CUT" strips on the model surface close to the leading edge of wing elements to fix the boundary layer transition position. Each strip is glued on the model surface and consists in a row of circular dots (disk roughness) of 1.27 [mm] (0.05[inch]) diameter, 0.29 [mm] (11.4 [mil inch]) height, placed every 2.54 [mm] (0.10[inch]) as shown in the Table 17 and Figure 26. Positions of strips were determined as same as NASA 10% preliminary CRM-HL model at QinetiQ in HLPW4 and those heights were determined based on the NACA report and KHI experience (Ecosystem team experience at QinetiQ and approach distance from stagnation point were also considered).

				Position					
Component				NASA /QinetiQ	KLWT		NOTE		
Component				10% Scale (NASA preliminary )	3.23% Scale (KHI CRM-HL)	(% of Refrence length)	NOTE		
		Inboard	283.9	28.4	9.2	3.6%Cref			
Wing	Upper	Mid board	285.6	28.6	9.2	3.6%Cref	Cref:Local coard length Trip dots were applied only area without slat		
		Outboard	133	13.3	4.3	1.7%Cref	The does were applied only area without		
	Lower	•	None	None	None	None	Not applicable		
F la	Тор		237.6	23.8	7.7	0.2%LFS	LEC-L		
Fuselage	Side		169.9	17.0	5.5	0.2%LFS	LFS:Length of Fuselage		
Nacelle	Outer su		153.0	13.3	4.9	2.3%LNC	LNC:Length of Nacelle		
D. I.	Тор		125.5	12.6	4.1	-			
Pylon	Side		None	None	None	None			
	Inboard	Inboard		None	None	None	Not applicable		
Flap Track Fairing (FTF)	Middle	Middle		None	None	None			
(111)	Outboan	d	None	None	None	None			
Horizontal Tail	Upper		-	-	(10%CHT)	-			
(HT)	Lower		-	-	(10%CHT)	-	CHT:Local chord length of Horizontal tail		
-	4	Wing 9.2 [	Inboard、 mm]			Fusela 7.7 [m	ge nm]		

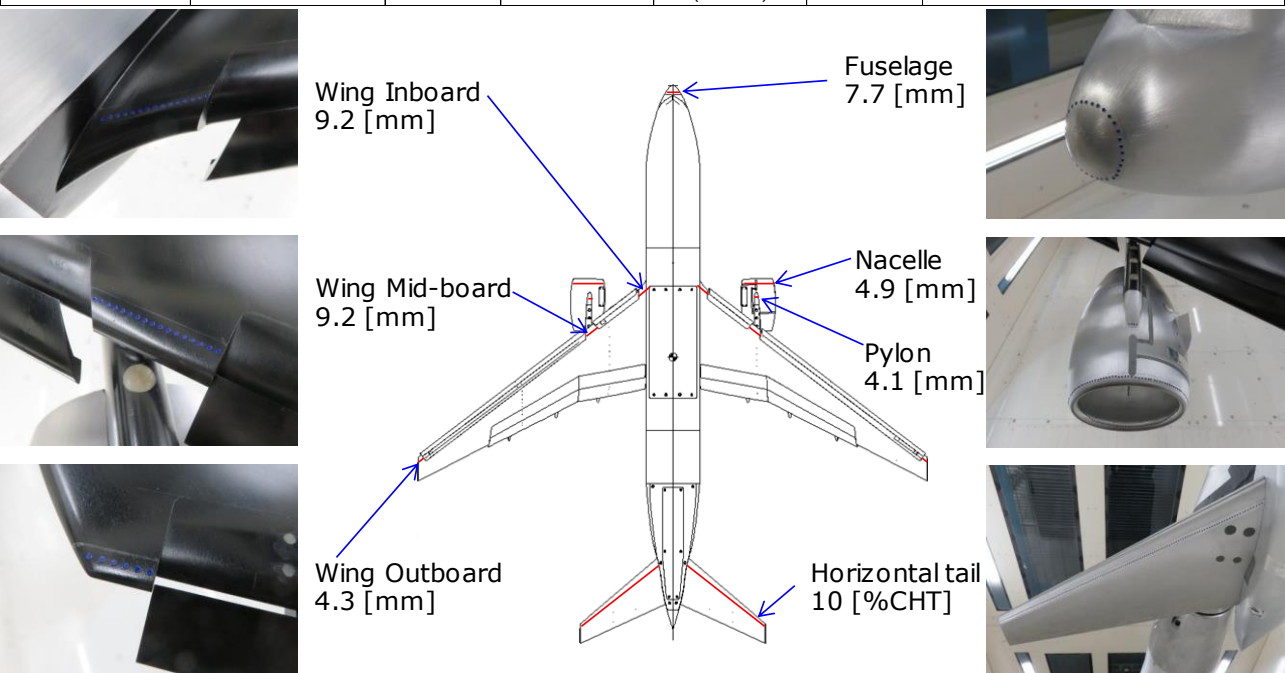


Figure 26– KHI CRM-HL model transition fixation positions in the 2<sup>nd</sup> testing campaign

# (B) Gap measurements

After model assembly, gap inspection was done to confirm the assembled model condition.

Both gap between slat and wing under slat surface and gap between flaps and wing trailing edge were measured by the block gauge with resolution (0.08 [mm] = 0.003 [inch]). Measured positions and the measurement results are shown in Figure 27. In the graph, designed values (black mark) and values measured at model factory (blue mark) are also shown in addition to the actual values measured at KLWT (red mark). These graphs show the reality of the model assemble repeatability and the difference between three values seems basically reasonably small.

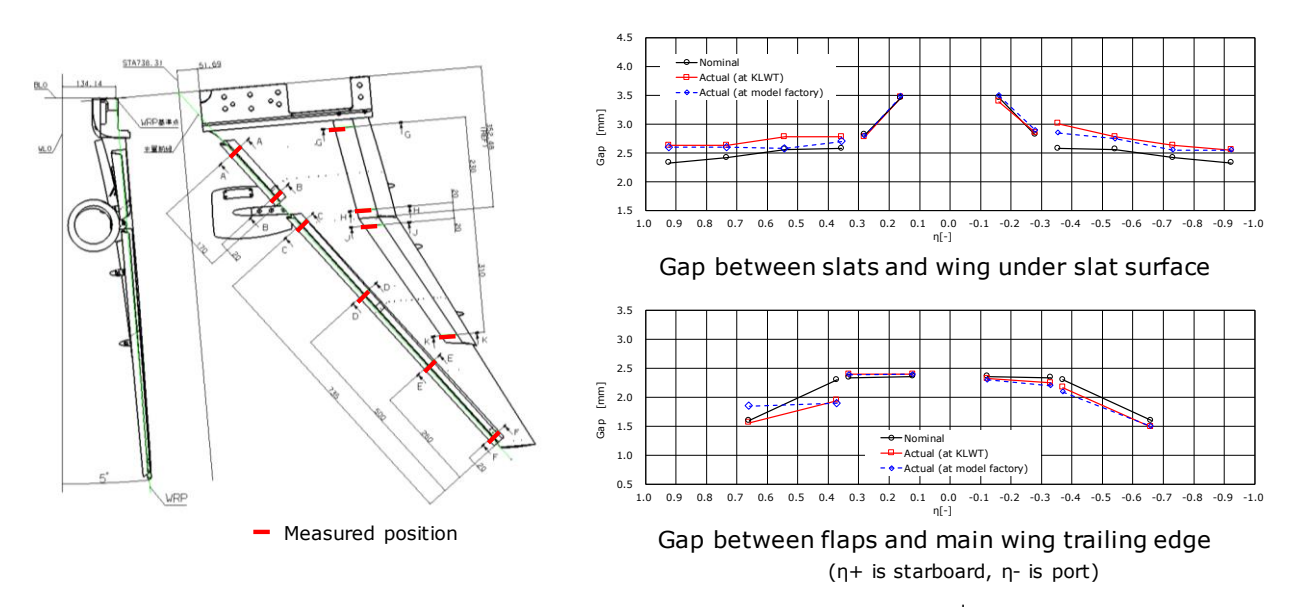


Figure 27– Flap gap condition of the KHI CRM-HL model in the 2<sup>nd</sup> testing campaign

# (C) Flap gap seal

Gap between inboard flap and outboard flap was sealed as shown in Figure 28.

Upper surface side of the flap gap was filled with clay(wax) and the step between flaps was smoothed up. Lower side of flap gap was sealed (covered) by the aluminum tape. In the 2<sup>nd</sup> testing campaign two gap seal configurations were tested. 1<sup>st</sup> configuration was based on the ONERA information and used for first 6 cases. 2<sup>nd</sup> configuration was based on the Ecosystem team information and this configuration is as same as the NASA 10% model testing at QinetiQ.



Gap seal configuration 1 (A64W001 - A64W006) (ONERA 1/19.5 style)



Gap seal configuration 2 (A64W007 - A64W038) (Ecosystem style) Figure 28– Flap gap seal of the KHI CRM-HL model

# (D) Model finish

After leak check of the pressure tubes, tapes are applied to the hole for fasteners and parts boundaries as shown in Figure 29.



Figure 29- KHI CRM-HL model finish under wing

CRM-HL Ecosystem team members from NASA and Boeing visited at KLWT on 6<sup>th</sup> to 13<sup>th</sup> Jan. 2023 to observe the 2<sup>nd</sup> testing campaign. They thoroughly verified the model finish conditions including trip position, flap gap seal and surface finishing, before wind-on testing as shown in Figure 30.

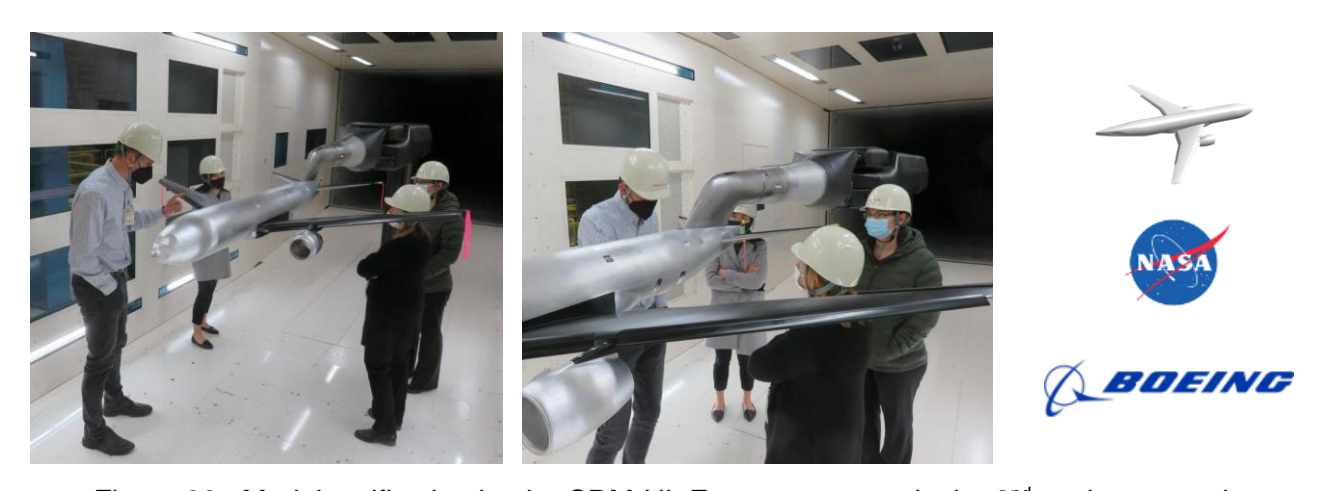


Figure 30– Model verification by the CRM-HL Ecosystem team in the 2<sup>nd</sup> testing campaign

# (E) Model tare

After model surface finish and before the wind-on testing, balance signals were acquired at several roll angles without wind condition for each configuration, and then, those values were used to calculate and determine the model tare weight and the position of the model center of gravity. In this testing, model tares were determined only for the configuration with horizontal tail (HT) and that without HT, and both configurations was with chine. (Chine off effect for tare was ignored.) Figure 31 shows two configurations of the KHI CRM-HL model in the 2<sup>nd</sup> testing campaign.



KHI CRM-HL with Horizontal tail



KHI CRM-HL without Horizontal tail

Figure 31– KHI CRM-HL model in KLWT in the 2<sup>nd</sup> testing campaign (Jan. 2023)

## 4.3.3 Test results

After model preparation, wind-on data sets were acquired. Table 18 shows the test conditions and model configurations for all wind-on data sets in the 2<sup>nd</sup> testing campaign. All data sets were acquired with the non-moving model (Pitch & Pause manner) at both wind-off and wind-on condition. For the force and pressure measurements, typical range of alpha was from -10 to 22 degrees with no side slip angle. During the measurements, the sting support system changed the model attitude, keeping the model center at the centerline of the test section of the wind tunnel adjusting the vertical position. Measured balance signals were transformed to the tentative dimensional loads (force [N] and moment [Nm]) using the balance matrix to correct the interactions between balance signals of 6 components. Aerodynamic loads for the model were derived from those tentative loads subtracting the model tare effect at each model attitude using the model weight and position of model center of gravity. For this data reduction, model attitude corrected for the model/support deflection was used. Regarding the moments, reference position was changed from the balance center to the moment reference point. Dynamic pressure was calculated from the total pressure measured at the setting chamber and static pressure measured at the static port on the wind tunnel side wall. This value was transformed to the value at model position using flow calibration curve acquired in the flow calibration process of KLWT, and corrected for the model blockage effects inside the closed test section.

Non-dimensional aerodynamic coefficients were derived from the above aerodynamic loads using the corrected dynamic pressure and the reference quantities as shown in Table **19**. All aerodynamic coefficients shown in the following pages are fully corrected for the wall interference such as induced angle effect and buoyancy effect by classical method, but not corrected for the support interference.

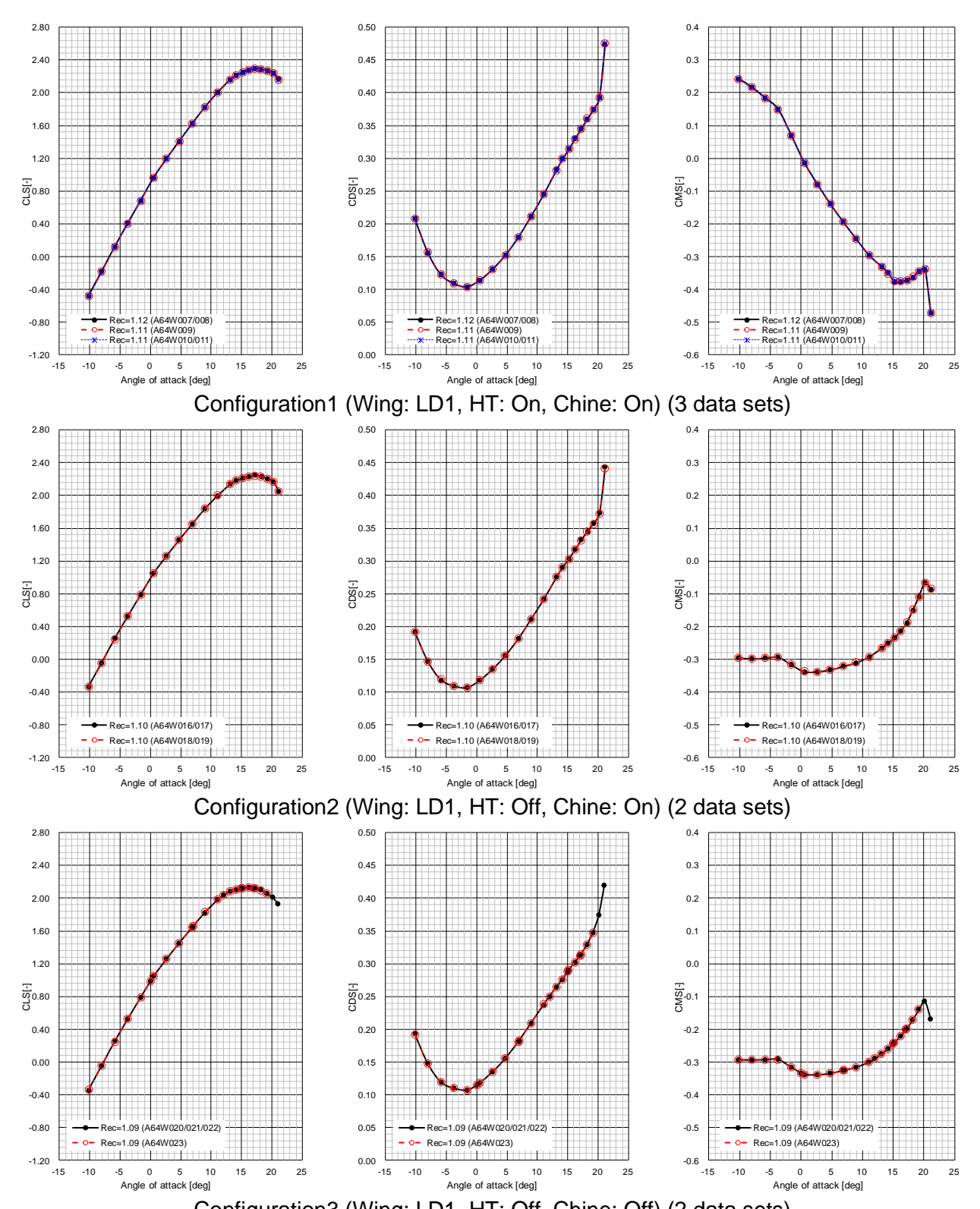
Table 18– Test conditions for the formal data acquisition in the 2<sup>nd</sup> testing campaign

	lable	e 18-	- res	t con	ditior	ns for	the 1	orma	al dat	a acc	quisiti	ion in	tne	9 2'	'" te	esting	campaign
Date	Run#	V	Mach Rec		AC	DA	Wing	нт	Chine	Trip	Trip Tuft	Flap GAP	Mea	suren	nent	Judge	Information
Dute	Ruii#	[m/s]	[-]	[*10 <sup>6</sup> ]	[deg]	[deg]	wing		Cillic	ШР	ruic	Sealing	Force	Press	Visualization	Juage	Thomaton
	A64W001 0-8	0-85	0-0.25	0-1.4	0	0										ОК	Test Run(Model check)
	A64W002	68	0.20	1.1	-10	20										ОК	
6-Jan-23	A64W003	68	0.20	1.1	-10	Х				OFF		A				NG	System stop
0-Jaii-23	A64W004	68	0.20	1.1	-10	Х			A				NG	System stop			
	A64W005	68	0.20	1.1	-10	Х										NG	System stop
	A64W006	68	0.20	1.1	-10	20										ОК	Repeatability
	A64W007	68	0.20	1.1	-10	2										ок	
	A64W008	68	0.20	1.1	2	20		ON								ОК	
	A64W009	68	0.20	1.1	-10	20										ок	
	A64W010	68	0.20	1.1	-10	12			ON							ОК	System stop
	A64W011	68	0.20	1.1	12	20										ОК	
	A64W012	78	0.23	1.3	-10	20					OFF		0	0	NA	ОК	
	A64W013	85	0.25	1.4	-10	20										ОК	
	A64W014	34	0.10	0.5	-10	19										OK	System stop
11-Jan-23	A64W015	34	0.10	0.5	-10	20										OK	
	A64W016	68	0.20	1.1	-10	14										ОК	System stop
	A64W017	68	0.20	1.1	14	20										ОК	
	A64W018	68	0.20	1.1	-10	17										ОК	System stop
	A64W019	68	0.20	1.1	17	20	LD1									ОК	
	A64W020	68	0.20	1.1	-10	15	LDI									ОК	System stop
	A64W021	68	0.20	1.1	15	18										ОК	System stop
	A64W022	68	0.20	1.1	18	20				ON		В				ОК	
	A64W023	68	0.20	1.1	-10	18			OFF	ON		В				ОК	System stop
	A64W024	68	0.20	1.1	7	20			UFF							ОК	
	A64W025	68	0.20	1.1	7	20										ОК	
12-Jan-23	A64W026	68	0.20	1.1	7,9,1	11,12					ON				Tuft	ОК	
	A64W027	68	0.20	1.1	15,16	,17,21		OFF								ОК	
	A64W028	68	0.20	1.1	7,12,15,	16,17,21										ок	
	A64W029	0	0.00	0.0	1	.7										ОК	Sequence check
	A64W030	68	0.20	1.1	1	.7										OK	Oil characteristic check
	A64W031	68	0.20	1.1	1	.7			ON				(0)	(0)		ОК	Oil characteristic check
	A64W032	68	0.20	1.1	1	.7										ОК	Sequence check
13-Jan-23	A64W033	68	0.20	1.1	1	.7					OFF				Oil	ОК	
13-1011-52	A64W034	68	0.20	1.1	2	1					OFF				OII	OK	
	A64W035	68	0.20	1.1		7										OK	
	A64W036	68	0.20	1.1	1	6		OFF							ОК		
	A64W037	68	0.20	1.1	1	.5									ОК		
	A64W038	68	0.20	1.1	1	.7										OK	

Table 19– Reference quantities in the 2<sup>nd</sup> testing campaign

			Data reduction	n reference	quantities					
Item		Symbol	KHI CRM-HL			Reference		NOTE (NASA 2.7% values from AIAA-2008-6919)		
			KIII CKM-IIL	NASA 5.2%	NASA 2.7%	Full Scale	Unit	Full Scale	Unit	,
Model Scale		Scale	3.23	5.20	2.70	100.00	[%]	100.00	[%]	
Reference Area		S <sub>ref</sub>	0.400299	1.037497	0.279710	383.690	[m <sup>2</sup> ]	594720	[in <sup>2</sup> ]	
Reference length	Longitudinal	C <sub>ref</sub>	0.22627	0.36428	0.18914	7.005	[m]	275.8	[in]	Mean aerodyamic chord
Reference length	Side/directional	b <sub>ref</sub>	1.89804	3.05567	1.58660	58.763	[m]	2313.5	[in]	62.46 [inch] for NASA 2.7% model (No cap)
		$X_{ref}$	1.08779		0.90929		[m]	33.7	[in]	35.799 [inch] aft for NASA 2.7%
Moment Reference (25%MAC position)		Y <sub>ref</sub>	0.0000		0.0000		[m]	0.0	[in]	On the fuselage centerline
(257011110 posicion)		Z <sub>ref</sub>	-0.06199		-0.05182		[m]	-1.9	[in]	2.04[inch] lower for NASA 2.7%
	X <sub>bal</sub>	1.01182				[m]				
Balance Center	Y <sub>bal</sub>	0.0000	0000				1.835[m] from sting interface plane			
	Z <sub>bal</sub>	0.01857				[m]				

Force measurement results of 3 configurations with LD1 wing at Mach number: M=0.20 and Reynolds number: Rec = 1.1 [\*10<sup>6</sup>] are shown in Figure 32. These figures show the longitudinal characteristic of the KHI CRM- HL only. For each configuration, more than two data sets were acquired to confirm the short-term repeatability within the 2<sup>nd</sup> testing campaign, and it seemed reasonably good basically.



Configuration3 (Wing: LD1, HT: Off, Chine: Off) (2 data sets)
(In the high AOA area, there are missing points due to the system error)
Figure 32– Typical force measurement results (Repeatability) in the 2<sup>nd</sup> testing campaign

To confirm the repeatability of the data a little more quantitatively, differences between  $N^{th}$  ( $N \ge 2$ )data and  $1^{st}$  data at each AOA are calculated and shown in Figure 33 for three configurations. (In this calculation AOA difference at each point was ignored since those are less than 0.004 [deg]) As shown in the figure, in small AOA (-5 to +10 [deg]) where the flow separation is limited over the wing, those differences are basically small, and those are less than  $\pm 3$  drag count in CD especially. In high AOA where flow separation increases, differences also increase but those are still not large.

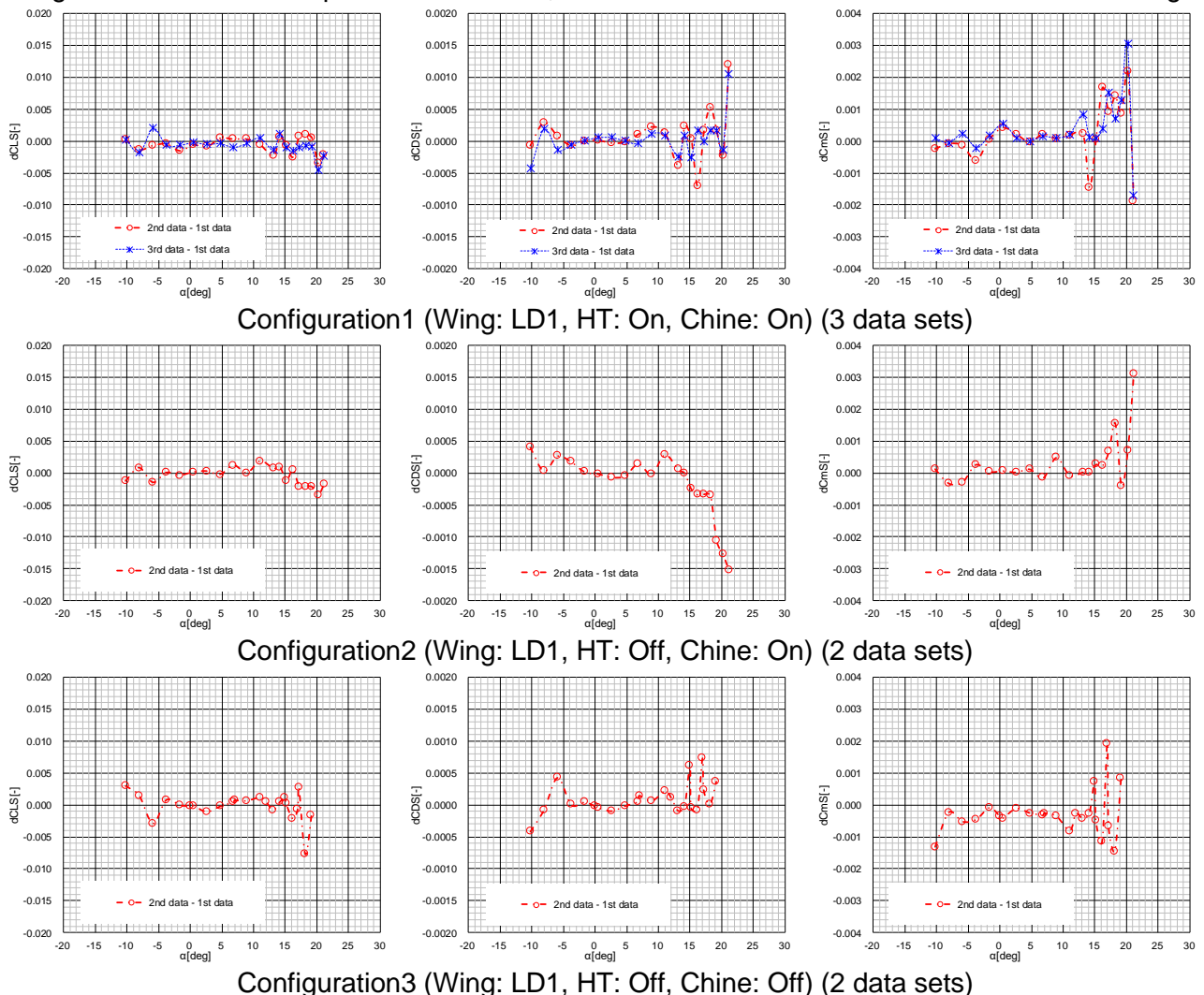


Figure 33– Data difference in the repetitive measurements (1st data is the reference)

Only for the configuration1 (Wing: LD1 HT on and Chine on), data difference between N<sup>th</sup> (N=1 to 3) data and average of 3 data samples at each alpha position are calculated and shown in Figure 34.

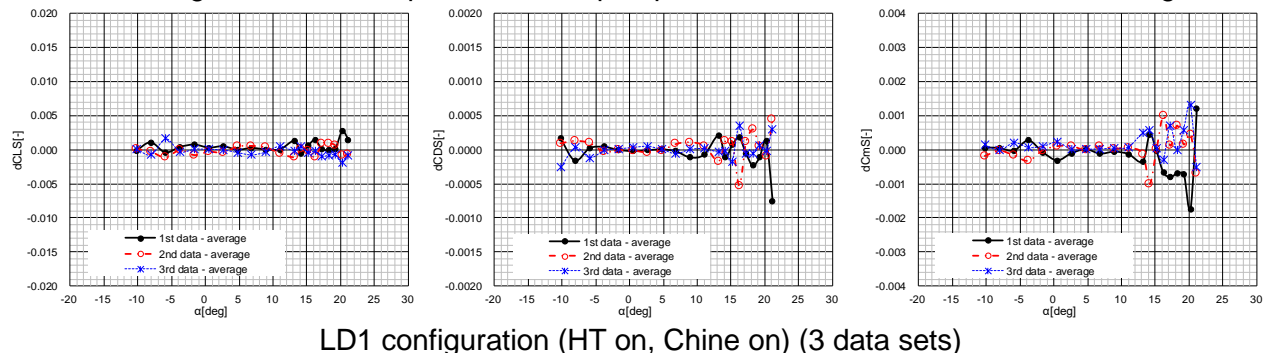


Figure 34– Data difference in the repetitive measurements (Average data is the reference)

Horizontal tail (HT) effect and Chine effect are shown in Figure 35. As shown in the figures, both component effects at M=0.20 and Rec=1.1 [\*10<sup>6</sup>] condition are properly acquired at KLWT.

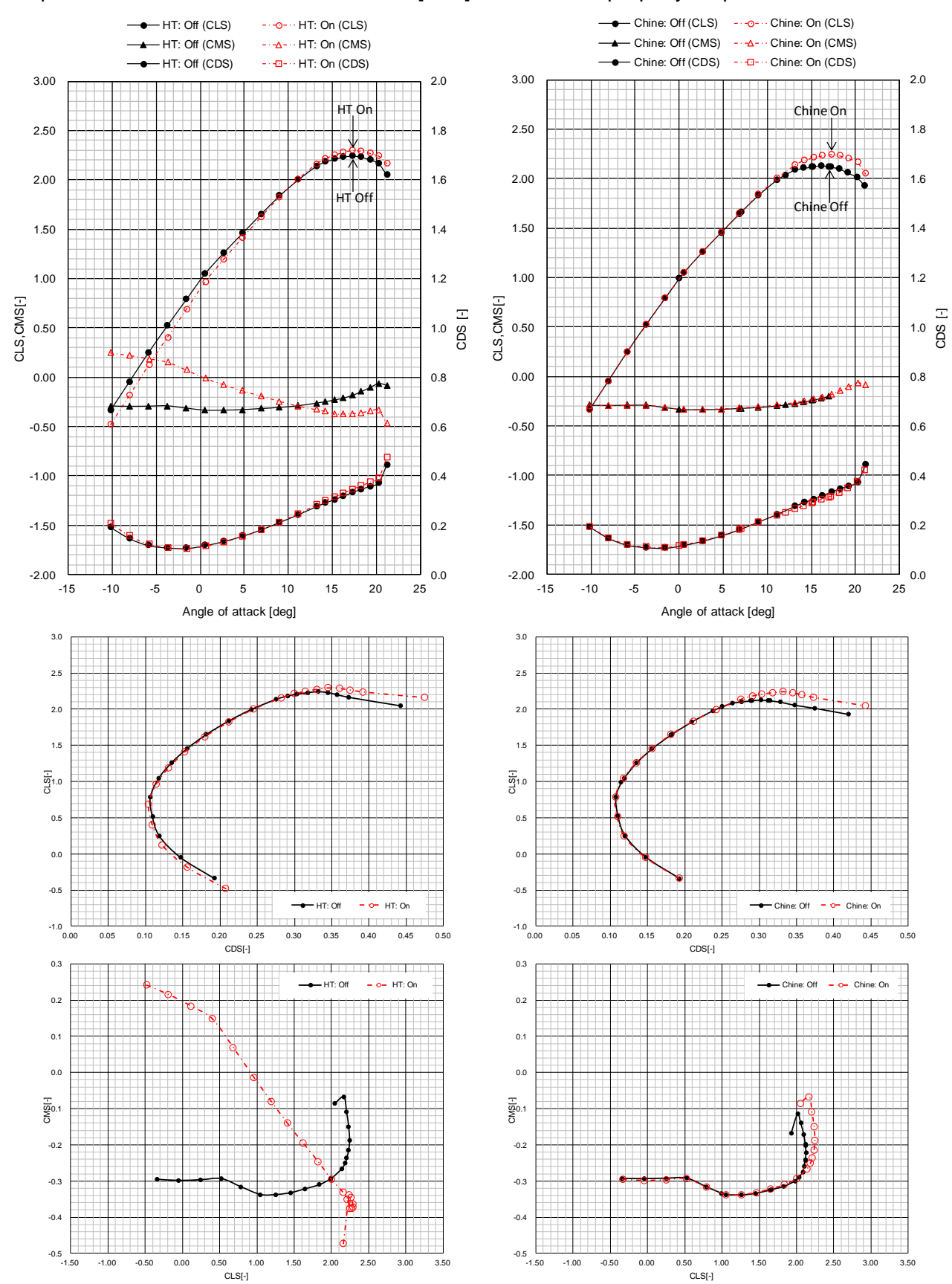


Figure 35– Representative force measurement results (Horizontal tail and Chine effect)

Regarding the chine effect, Figure 36 shows the flow visualization results with tufts, that includes backside area of the nacelle/pylon. As shown in the figure, chine works to prevent the flow separation backward of pylon even in the Rec =  $1.1 [*10^6]$  condition at KLWT.

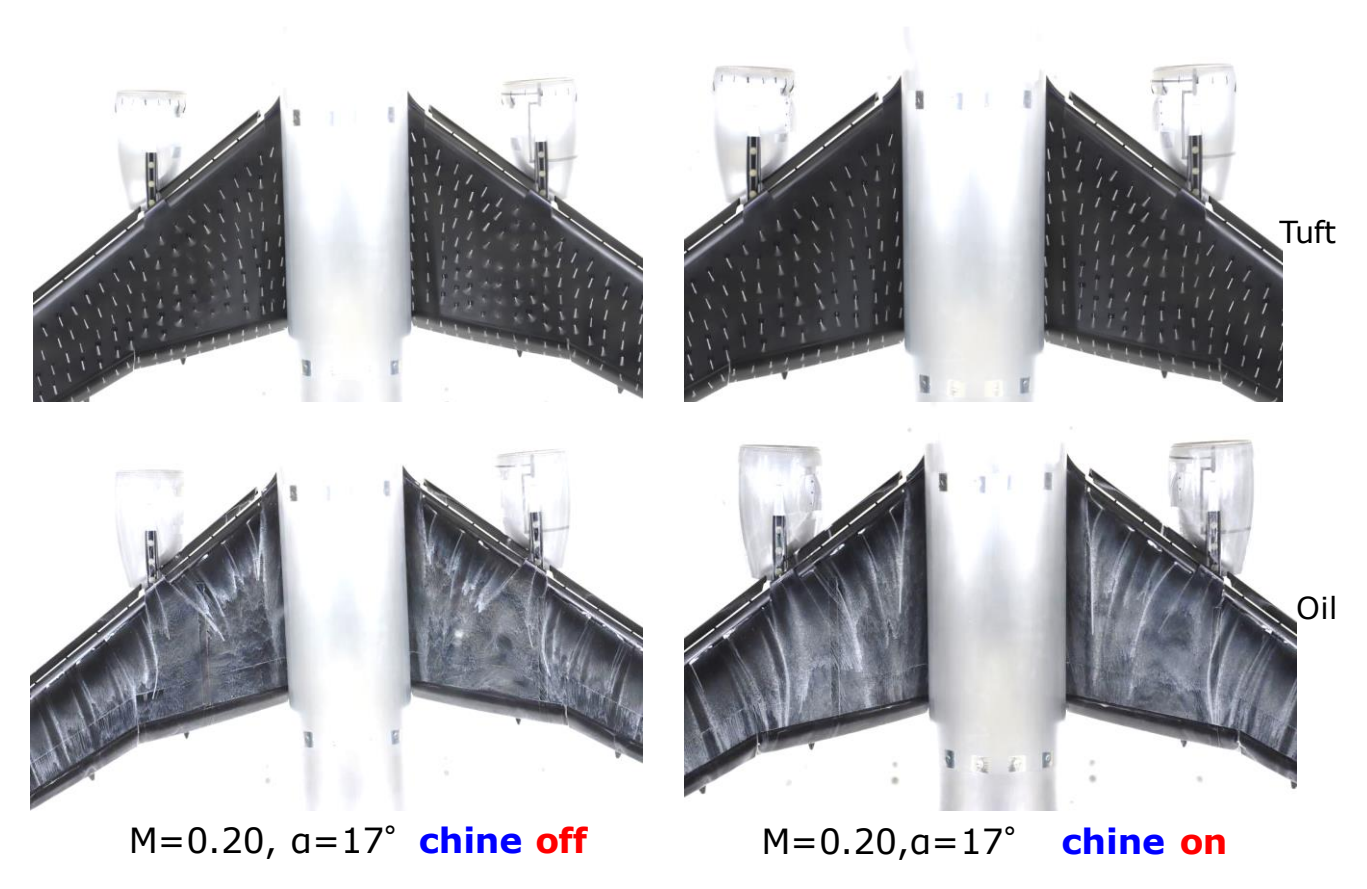
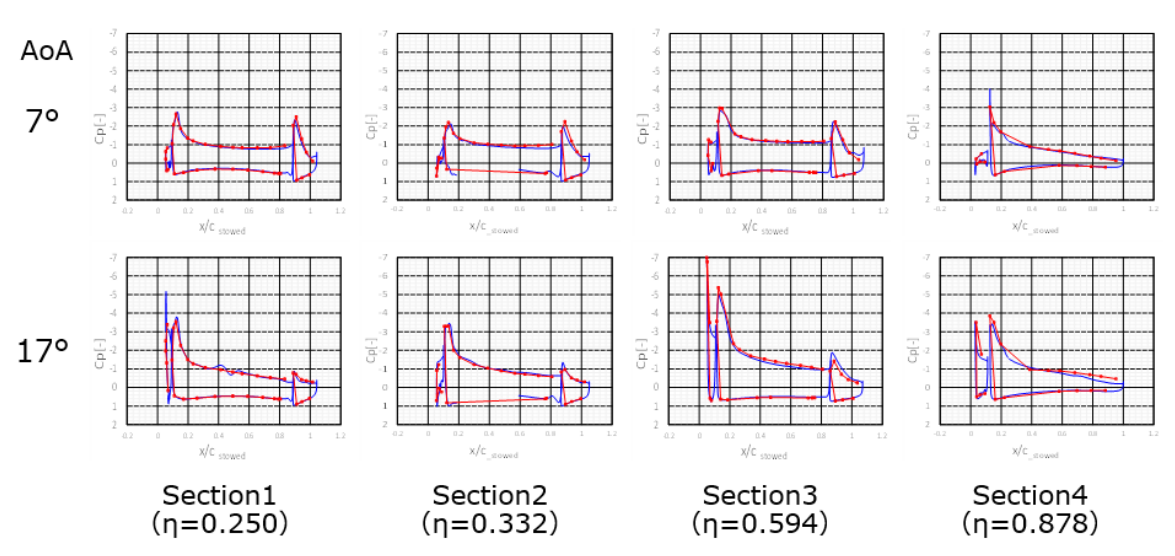


Figure 36– Representative visualization results (top: tuft, bottom oil)

Typical pressure measurements are shown in the figure below.



CFD (EQ:RANS steady, Turbulence model; SA-noft2-R-QCR, Cell:100M, KHI in house code Cflow)

Cp comparison (M=0.20,LD1,Chine-off,Main Wing, AoA 7°, 17°) Rec=1.1M

Figure 37– Representative pressure measurement results (Red: WT, blue: CFD)

## 4.3.4 CFD results

Test results shown in this paper was not corrected for the support interference effect. In order to assess the support effect and wall interference, following CFD analyses were done after the testing.

# (A) Blade sting effect

Firstly, in order to confirm the effect of the blade sting used for the testing, two model shapes shown in Figure 38 were prepared and flow fields around these models at M=0.20 and Rec=1.07\*10<sup>6</sup> were calculated using KHI in-house code with the conditions shown in Table **20**. Table **21** describes the model configuration in detail, and Figure 39 shows the CFD results for these models, and we found that the blade sting has almost no effect on the aerodynamic characteristics of KHI-CRM-HL model.

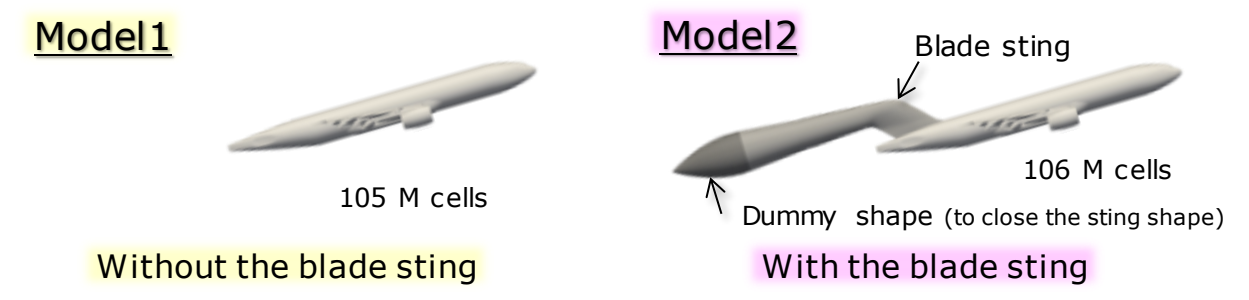


Figure 38– Model shapes for CFD analysis to confirm the blade sting effect

Table 20– CFD conditions for the blade sting effect confirmation

Governing Equations	Reynolds-averaged Navier-Stokes equations (RANS)					
Spatial discretization	Cell-centered finite volume method					
Flux reconstruction	2 <sup>nd</sup> -order accurate reconstruction based on MUSCL					
Inviscid flux	Simple low-dissipation AUSM scheme (SLAU)					
Viscous flux	2 <sup>nd</sup> -order accurate central difference					
Turbulence model	Spalart-Allmaras one-equation model (SA-noft2-QCR2000-R)					
Time integration	Matrix-free Gauss Seidel (MFGS) implicit method					
Software	Cflow (KHI original)					

Table 21– CFD model configurations for the blade sting effect confirmation

Model Name	KHI CRM-HL		Config.	Landing (Nominal = LD1)						
Model Shape	CRM-HL reference configuration	Wing	Slat angle	30 [deg]						
Model Scale	3.23 [%]	vvirig	Inboard Flap angle	40 [deg]						
Blade sting	Off (Model1) / On (Model2)		Outboard Flap angle	37 [deg]						
Vertical tail	Off	Nacelle/Py	lon	On						
Horizontal tail	Off	Nacelle ch	ine	On						
Landing Gear	Off	Flap Track	Fairing	NASA style (not hinged ver.)						

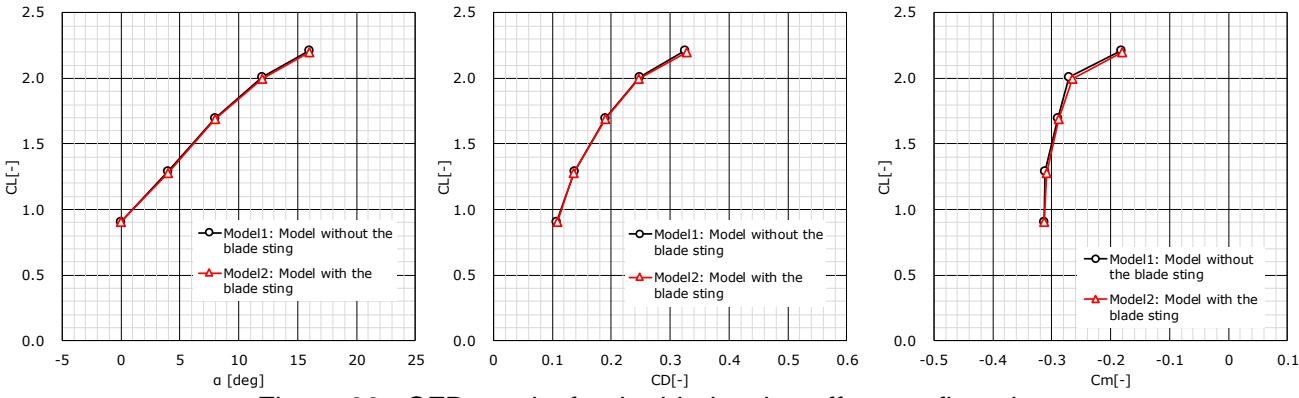


Figure 39– CFD results for the blade sting effect confirmation

## (B) Wall effect

Secondly, in order to confirm the effect of the test section wall, additional model was made as shown in Figure 40 and flow fields around this model at same flow condition was also calculated with same CFD parameters. Flow calibration data for KLWT was used to set the Mach number in the test section properly. Figure 41 shows the CFD result with wall and without wall. As shown in this figure, the result with wall has steeper lift slope than the result without wall, and optimistic drag-polar since the wind tunnel wall induced the upwash around the wing. Figure 42 shows the comparison between CFD and WT results. Especially center figure shows the WT result with and without wall correction, and the right figure shows the direct comparison of CFD and WT results. These figures show that there is a slight shift between CFD and WT results, but CFD captured the basic aerodynamic trend of the KHI CRM-HL at this condition, and the wall effect correction for the WT result is basically reasonable both qualitatively and quantitively except stall region.

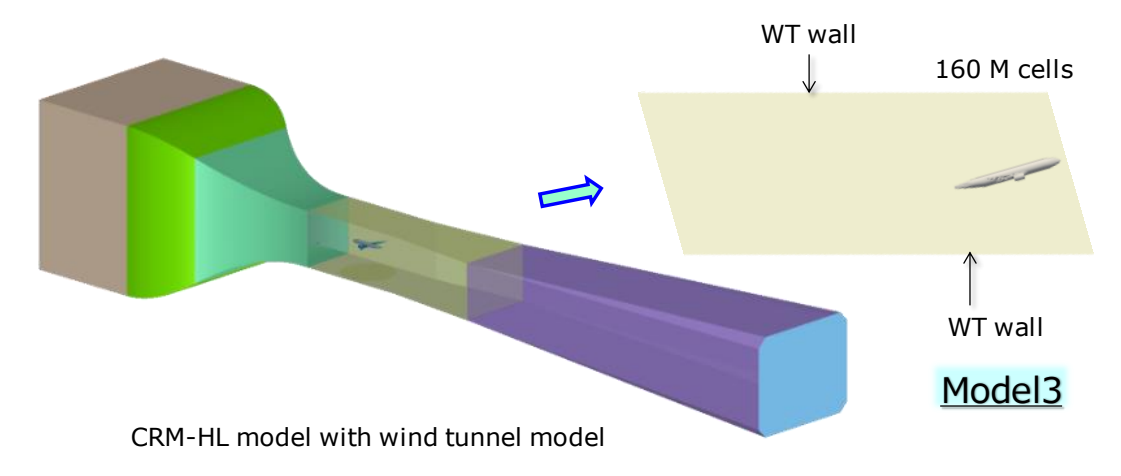


Figure 40- Model shapes for CFD analysis to confirm wall effect

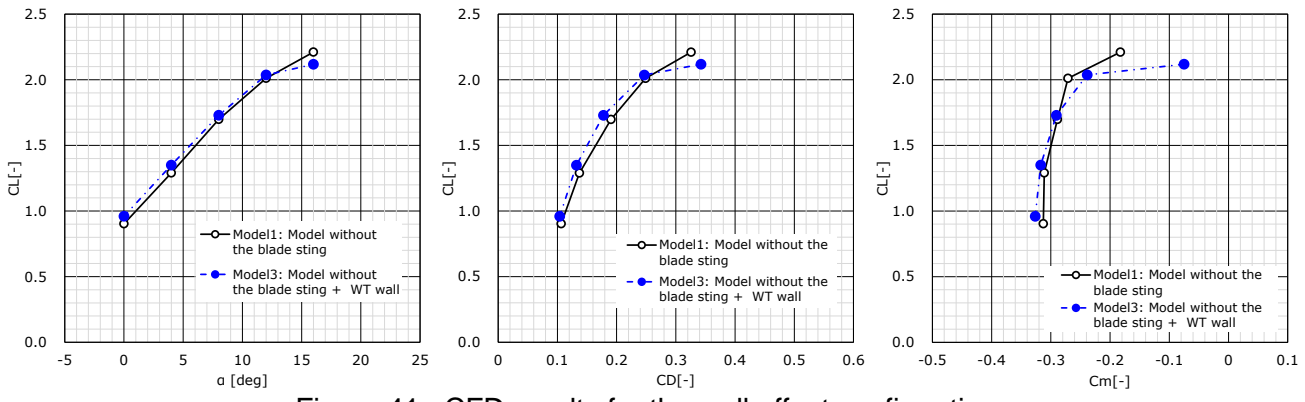


Figure 41– CFD results for the wall effect confirmation

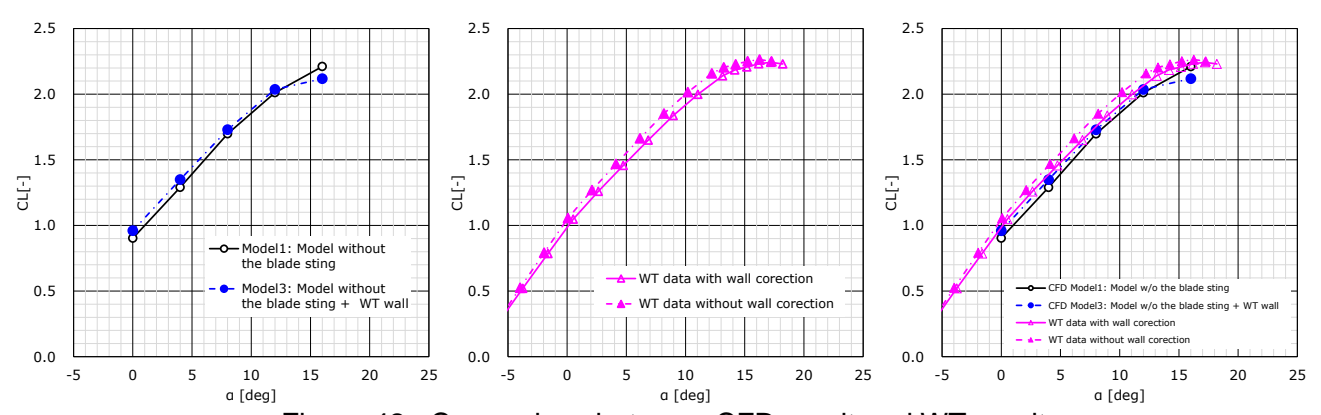
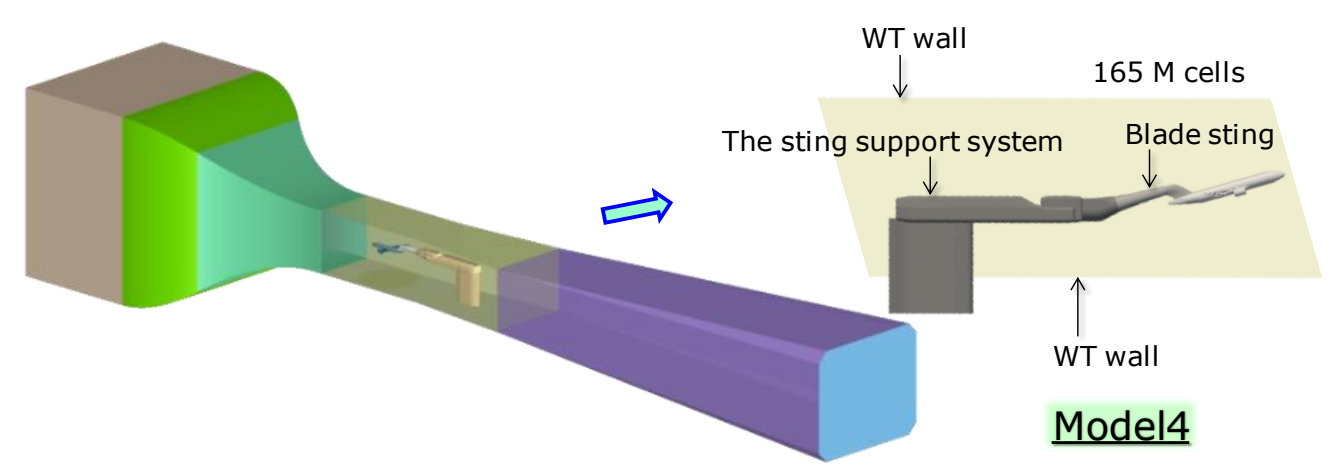


Figure 42– Comparison between CFD result and WT result

# (C) Support system effect

Finally, in order to confirm the effect of the sting support system (relatively large blockage effect), additional model was made as shown in Figure 43 and flow fields around this model at same flow condition was also calculated with same CFD parameters. Figure 44 shows the CFD result with and without the sting support system. As shown in this figure, there is almost no effect of the sting support system effect in the small alpha region, and the support system effect appears at only high alpha(lift) region. This result might suggest that the WT result with the sting support system at KLWT is basically free from the support system effect or interference in the small alpha region, but it has some influence in the high alpha condition, so it is necessary to conduct the support system correction in some way. But CFD result in high alpha region still has relatively large uncertainty, so more detail confirmation and calculation will be necessary to conclude on this issue.



CRM-HL model with blade sting, the sting support system, and wind tunnel model

Figure 43– Model shapes for CFD analysis to confirm the sting support system effect

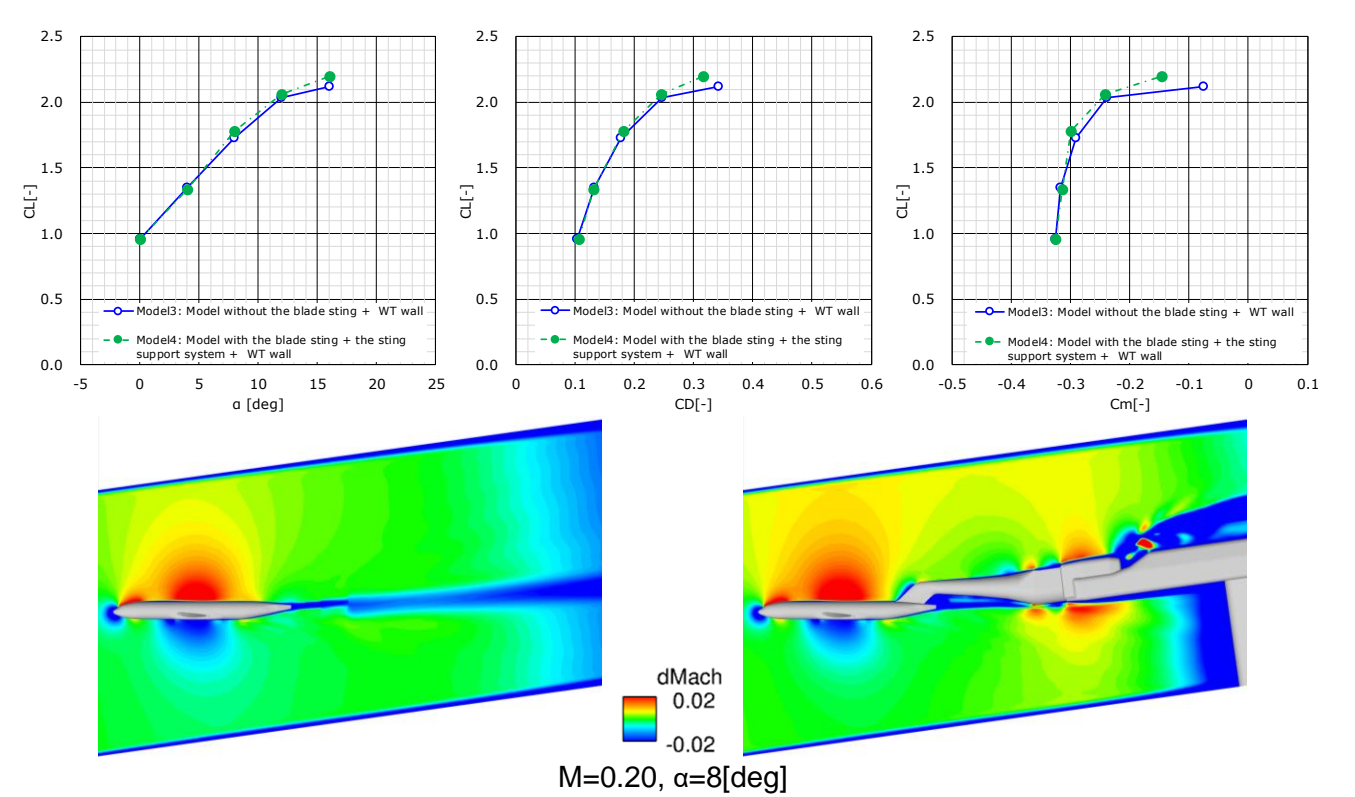


Figure 44– CFD results for the sting support system effect confirmation

# 5. Summary/Future plan

KHI built the new low-speed aero-acoustic wind tunnel (KLWT) in 2017-2019 and introduced KHI CRM-HS/KHI CRM-HL models as a check standard model for KLWT. So far two testing campaigns were done in 2022 -2023 and some of the measured data is shown in this paper. In the future, KHI will analyze the uncertainty of the measurement data at KLWT. Since KHI introduced the KHI CRM-HL as a check model, at least one testing campaign will happen every two year, so it is possible for KHI to add some more data of KHI CRM-HL. In the future testing campaign, model deformation data and flow field data will be acquired using existing optic cameras and PIV instruments.

Activities of the Ecosystem clearly shows the current edges and limitations of CFD and EFD in the world, and mutually complimentary relationship between CFD and EFD, suggesting the necessity of continuous efforts to improve both technologies for the future sustainable developments of novel aircrafts. Since those activities also teach us our current status and limitations clearly, KHI will also try to improve and expand both CFD/EFD techniques until now and from now on to continue to develop environment friendly aircrafts at the edge of the world, participating in the Ecosystem and hoping our actions will help team some day in the future.

# 6. Acknowledgements

KHI fully appreciates all supports and friendship of the CRM-HL Ecosystem and its members. KHI team members are very grateful to JAXA engineers, especially Norikazu Sudani and Masataka Kohzai for their supports in the introduction process of KHI CRM-HS and sharing the wind tunnel data for comparison. KHI team also would like to specially thank Melissa Rivers who is one of the leaders of the CRM project and let KHI join the Ecosystem kindly, Jeffrey Slotnick who led and established the Ecosystem, Doug Lacy who developed the CRM-HL and support our model design work, and Martin Wright, who was an test engineer at ETW, encouraged the author not only in my young days but also in the web meetings of this Ecosystem with chats and E-mails. This paper is a heartfelt tribute to Martin who supported KHI and other aircrafts developments through the high-quality cryogenic testing with amount of advice and smiles and passed away last year suddenly.

## 7. Contact Author Email Address

mailto: hashioka\_takahiro@global.kawasaki.com

# 8. Copyright Statement

The authors confirm that they, and/or their company or organization, hold copyright on all of the original material included in this paper. The authors also confirm that they have obtained permission, from the copyright holder of any third party material included in this paper, to publish it as part of their paper. The authors confirm that they give permission, or have obtained permission from the copyright holder of this paper, for the publication and distribution of this paper as part of the ICAS proceedings or as individual off-prints from the proceedings.

## **Nomenclature**

 $\alpha$  [deg] : Angle of Attack (AOA)  $\beta$  [deg] : Angle of Sideslip M [-] : Mach Number V [m/s] : Flow speed

Rec [-] : Reynolds number based on the model reference length

Q [Pa] : Dynamic pressure of the uniform flow PS [Pa] : Static pressure of the uniform flow P [Pa] : Local pressure on the model surface Cp [-] : Pressure coefficient (Cp = (p-PS)/Q)

b [m] : Wing span

c<sub>ref</sub> [m] : Model reference length for longitudinal characteristicsb<sub>ref</sub> [m] : Model reference length for side/directional characteristics

 $\begin{array}{cccc} S_{\text{ref}} & & [m] & : \text{Model reference area} \\ W & & [m] & : \text{Width of the test section} \\ H & & [m] & : \text{Height of the test section} \\ \eta & & [-] & : \text{Wing semi-span ratio} \\ \end{array}$ 

FX [N] : Force vector component in the x direction of the balance axis
FY [N] : Force vector component in the y direction of the balance axis
FZ [N] : Force vector component in the z direction of the balance axis

MX [Nm] : Moment around x direction of the balance axis
MY [Nm] : Moment around y direction of the balance axis
MZ [Nm] : Moment around z direction of the balance axis

CDS [-] : Drag coefficient in stable axis
CLS [-] : Lift coefficient in stable axis

CMS [-] : Pitching moment coefficient in stable axis CYS [-] : Side force coefficient in stable axis

CIS [-] : Rolling moment coefficient in stable axis
CNS [-] : Yawing moment coefficient in stable axis
(Xref, Yref, Zref) [m] : Moment reference point in CATIA axis

(X<sub>bal</sub>, Y<sub>bal</sub>, Z<sub>bal</sub>) [m] : Balance center in CATIA axis

# Abbreviation/Acronym

CAD : Computer Aided Design
CFD : Computational Fluid Dynamics
EFD : Experimental Fluid Dynamics

WT : Wind Tunnel

HLPW: High Lift Prediction Workshop
CRM: NASA Common Research Model

CRM-HL: High Lift version CRM
CRM-HS: High Speed version CRM

NASA : National Aeronautics and Space Administration

BOEING : The Boeing Company

ONERA : THE FRENCH AEROSPACE LAB (Office National d'éludes et de Recherches Aérospatiales)

JAXA : Japan Aerospace Exploration Agency

QinetiQ : QinetiQ Group plc

PSI : The Pressure Systems Incorporated KHI : Kawasaki Heavy Industries, Ltd.

KLWT : Kawasaki Low-speed aero-acoustic Wind Tunnel

AOA : Angle of attack A/D : Analogue / Digital

LD : Landing
TO : Take Off
HT : Horizontal Tail
FTF : Flap Track Fairing

### References

- [1] Lacy, D. S. and Sclafani, A. J., "Development of the high lift common research model (HL-CRM): A representative high lift configuration for transonic transports," AIAA Paper 2016-0308, January 2016. doi:10.2514/6.2016-0308
- [2] Lacy, D. S. and Clark, A. M., "Definition of Initial Landing and Takeoff Reference Configurations for the High Lift Common Research Model (CRM-HL)," AIAA Paper 2020-2771, June 2020. doi:10.2514/6.2020-2771
- [3] Clark, A.M., Slotnick, J.P., Taylor, N. and Rumsey, C.L., "Requirements and Challenges for CFD Validation within the High-Lift Common Research Model Ecosystem," AIAA Paper 2020-2772, June 2020. doi:10.2514/6.2020-2772
- [4] Evans, A., Lacy, D., Smith, I. and Rivers, M., "Test Summary of the NASA Semi-Span High-Lift Common Research Model at the QinetiQ 5-Metre Low-Speed Wind Tunnel," AIAA Paper 2020-2770, June 2020. doi:10.2514/6.2020-2770
- [5] Fell, J., Webb, S.R., Laws, C.T., Snyder, M.L. and Rhew, R., "Development of the NASA 10% High-Lift Common Research Model (CRM-HL)," AIAA Paper 2021-0385, January 2021. doi:10.2514/6.2021-0385
- [6] Slotnick, J.P., "AVT-338 Research Specialists' Meeting on Advanced Wind Tunnel Boundary Simulation II The High-Lift Common Research Model Ecosystem," May 2021, AVT-RWS-340
- [7] Mouton, S., Charpentier, G. and Lorenski, A., "Test Summary of the Full-Span High-Lift Common Research Model at the ONERA F1 Pressurized Low-Speed Wind Tunnel," AIAA Paper 2023-0823, January 2023. doi:10.2514/6.2023-0823
- [8] Hood, Kolleen K., "Design of the 6% Boeing High Lift Common Research model (CRM-HL)," AIAA Paper 2023-0824, January 2023. Doi:10.2514/6.2023-0824
- [9] Slotnick, J.P., "A CFD Validation Ecosystem to Advance the Prediction of Low-Speed Aerodynamics" 34<sup>th</sup> Congress of International Council of Aeronautical Sciences, September 2024 (to be published).
- [10] Vassberg, J.C., DeHaan, M.A., Rivers, S.M. and Wahls, R.A., "Development of a Common Research Model for Applied CFD Validation Studies," AIAA Paper 2008-6919, August 2008. doi:10.2514/6.2008-6919
- [11] Rivers, S.M. and Dittberner, A., "Experimental Investigations of the NASA Common Research Model (Invited)," AIAA Paper 2010-4218, June 2010. doi:10.2514/6.2010-4218
- [12] Rivers, S.M., Quest, J. and Rudnik, R., "Comparison of the NASA Common Research Model European Transonic Wind Tunnel Test Data to NASA Test Data (Invited)," AIAA Paper 2015-1093, January 2015. doi:10.2514/6.2015-1093
- [13] Jones, A.M., Mejia, K.M., Ulk, C., Murahashi, Y., Nagata, T. and Ochi, A., "Comparison of PIV and CFD Measurements of an Advanced Supersonic Research Concept Model," AIAA Paper 2017-3639, June 2017. doi:10.2514/6.2017-3639
- [14] Yokokawa, Y., Murayama, M., Ito, Y., Ura, H., Kwak, D.-Y., Kobayashi, H., Shindo, S. and Yamamoto, K. "Noise Generation Characteristics of a High-lift Swept and Tapered Wing Model," in 19th AIAA/CEAS Aeroacoustics Conference, Berlin, 2013.
- [15] Murayama, M., Yokokawa, Y., Ito, Y., Yamamoto, K., Takaishi, T. and Ura, H., "Study on Noise Generation from Slat Tracks Using a High-Lift Wing Model," in 21st AIAA/CEAS Aeroacoustics Conference, Dallas, TX, 2015.
- [16] Murayama, M., Yokokawa, Y., Ito, Y., Yamamoto, K., Takaishi, T., Ura, H. and Hirai, T. "Study on Change of Noise Generation from Slat Track Shape," in 22nd AIAA/CEAS Aeroacoustics Conference, Lyon, 2016.
- [17] Ribeiro, A.F.P., Murayama, M., Ito, Y., Yamamoto, K. and Hirai, T., "Effect of Slat Tracks and Inboard Slat Tip Geometry on Airframe Noise," AIAA Paper 2022-2952, June 2022. doi:10.2514/6.2022-2952
- [18] Brodersen, O. and Stuermer, A. "Drag prediction of engine-airframe interference effects using unstructured Navier-Stokes calculations," AIAA Paper 2001-2414, June 2021. doi:10.2514/6.2001-2414
- [19] Uchiyama, T. Kohzai, M., Miki, H., Hirotani, T., Sudani, N. and Shutoku, H., "Experimental Investigation of a 160% Scaled NASA Common Research Model at Low Speed Conditions," AIAA Paper 2019-2190, January 2019, doi:10.2514/6.2019-2190